

Direction-oriented Multi-objective Learning: Simple and Provable Stochastic Algorithms

Peiyao Xiao[†], Hao Ban[‡], Kaiyi Ji^{†*}

[†]Department of CSE, University at Buffalo

[‡] Zuoyi Technology

{peiyaoxi, kaiyiji}@buffalo.edu, bhsimon0810@gmail.com

May 31, 2023

Abstract

Multi-objective optimization (MOO) has become an influential framework in many machine learning problems with multiple objectives such as learning with multiple criteria and multi-task learning (MTL). In this paper, we propose a new direction-oriented multi-objective problem by regularizing the common descent direction within a neighborhood of a direction that optimizes a linear combination of objectives such as the average loss in MTL. This formulation includes GD and MGDA as special cases, enjoys the direction-oriented benefit as in CAGrad, and facilitates the design of stochastic algorithms. To solve this problem, we propose Stochastic Direction-oriented Multi-objective Gradient descent (SDMGrad) with simple SGD type of updates, and its variant SDMGrad-OS with an efficient objective sampling in the setting where the number of objectives is large. For a constant-level regularization parameter λ , we show that SDMGrad and SDMGrad-OS provably converge to a Pareto stationary point with improved complexities and milder assumptions. For an increasing λ , this convergent point reduces to a stationary point of the linear combination of objectives. We demonstrate the superior performance of the proposed methods in a series of tasks on multi-task supervised learning and reinforcement learning. Code is provided at <https://github.com/ml-opt-lab/sdmgrad>.

1 Introduction

In recent years, multi-objective optimization (MOO) has drawn intensive attention in a wide range of applications such as online advertising Ma et al. (2018), hydrocarbon production You et al. (2020), autonomous driving Huang et al. (2019), safe reinforcement learning Thomas et al. (2021), etc. In this paper, we focus on the stochastic MOO problem, which takes the formulation of

$$\min_{\theta \in \mathbb{R}^m} \mathbf{L}(\theta) := (\mathbb{E}_{\xi}[L_1(\theta; \xi)], \mathbb{E}_{\xi}[L_2(\theta; \xi)], \dots, \mathbb{E}_{\xi}[L_K(\theta; \xi)]), \quad (1)$$

where m is the parameter dimension, $K \geq 2$ is the number of objectives and $L_i(\theta) := \mathbb{E}_{\xi} L_i(\theta; \xi)$. One important example of MOO in eq. (1) is the multi-task learning (MTL) Vandenhende et al. (2021); Sener &

*First two authors contributed equally.

Algorithms	Batch sizes	Nonconvex obj	Sample complexity	Objective sampling
SMG Liu & Vicente (2021)	$\mathcal{O}(\epsilon^{-2})$	✗	$\mathcal{O}(\epsilon^{-4})$	✗
MoCo Fernando et al. (2023)	$\mathcal{O}(1)$	✓	$\mathcal{O}(\epsilon^{-10})$	✗
SDMGrad (Corollary 1)	$\mathcal{O}(1)$	✓	$\mathcal{O}(\epsilon^{-8})$	✗
SDMGrad-OS (Theorem 2)	$\mathcal{O}(1)$	✓	$\mathcal{O}(\epsilon^{-8})$	✓

Table 1: Comparison of different algorithms for stochastic MOO with smooth nonconvex objectives.

Koltun (2018), which aims to solve an average loss for all K tasks as

$$\theta^* = \arg \min_{\theta \in \mathbb{R}^m} \left\{ \bar{L}(\theta) \triangleq \frac{1}{K} \sum_{i=1}^K L_i(\theta) \right\}, \quad (2)$$

where $L_i(\theta)$ is the loss function for task i . However, solving the MOO problem is challenging because it cannot find a common parameter θ that minimizes all individual objective functions simultaneously. As a result, a widely-adopted target is to find the *Pareto stationary point* at which there are no common descent direction for all objective functions. In this context, a variety of gradient manipulation methods have been proposed, including the multiple gradient descent algorithm (MGDA) Désidéri (2012), PCGrad Yu et al. (2020a) and CAGrad Liu et al. (2021). Among them, MGDA updates the model parameter θ using a time-varying multi-gradient, which is a convex combination of gradients for all objectives. CAGrad further improves MGDA by imposing a new constraint on the difference between the common descent direction and the average gradient to ensure the convergence to the minimum of the average loss of MTL. However, these approaches mainly focus on the deterministic case, and their stochastic versions still remain under-explored.

Stochastic MOO has not been well understood except several attempts recently. Inspired by MGDA, Liu & Vicente (2021) proposed stochastic multi-gradient (SMG), and established its convergence with convex objectives. However, their analysis requires the batch size to increase linearly. In the more practical nonconvex setting, Zhou et al. (2022) proposed a correlation-reduced stochastic multi-objective gradient manipulation (CR-MOGM) to address the non-convergence issue of MGDA, CAGrad and PCGrad in the stochastic setting. However, their analysis requires a restrictive assumption on the bounded function value. Toward this end, Fernando et al. (2023) recently proposed a method named MoCo as a stochastic counterpart of MGDA by introducing a tracking variable to approximate the stochastic gradient. However, their analysis requires that the number K of objectives is small at an order of $T^{\frac{1}{10}}$, where T is the number of iterations, and hence may be unsuitable for the scenario with many objectives. Thus, it is highly demanding but still challenging to develop efficient stochastic MOO methods with guaranteed convergence in the nonconvex setting under mild assumptions.

1.1 Our Contributions

Motivated by the limitations of existing methods, we propose Stochastic Direction-oriented Multi-objective Gradient descent (SDMGrad), which is easy to implement, flexible with a new direction-oriented objective formulation, and achieves a better convergence performance under milder assumptions. Our specific contributions are summarized as follows.

Algorithms	Nonconvex obj	Sample complexity	Objective sampling
CR-MOGM Zhou et al. (2022)	✓	$\mathcal{O}(\epsilon^{-4})$	✗
MoCo Fernando et al. (2023)	✓	$\mathcal{O}(\epsilon^{-2})$	✗
SDMGrad (Corollary 3)	✓	$\mathcal{O}(\epsilon^{-2})$	✗
SDMGrad-OS (Theorem 4)	✓	$\mathcal{O}(\epsilon^{-2})$	✓

Table 2: Comparison under an additional bounded function assumption.

New direction-oriented formulation. We propose a new MOO objective (see eq. (6)) by regularizing the common descent direction d within a neighborhood of a direction d_0 that optimizes a linear combination $L_0(\theta)$ of objectives such as the average loss in MTL. This formulation is general to include gradient descent (GD) and MGDA as special cases and takes a similar direction-oriented spirit as in CAGrad Liu et al. (2021). However, differently from the objective in CAGrad Liu et al. (2021) that enforces the gap between d and d_0 to be small via constraint, our regularized objective is easier to design near-unbiased multi-gradient, which is crucial in developing provably convergent stochastic MOO algorithms.

New stochastic MOO algorithms. The proposed SDMGrad is simple with efficient stochastic gradient descent (SGD) type of updates on the weights of individual objectives in the multi-gradient, and on the model parameters with (near-)unbiased (multi-)gradient approximations at each iteration. SDMGrad does not require either the linearly-growing batch sizes as in SMG or the extra tracking variable for gradient estimation as in MoCo. Moreover, we also propose SDMGrad-OS (which refers to SDMGrad with objective sampling) as an efficient and scalable counterpart of SDMGrad in the setting with a large number of objectives. SDMGrad-OS samples a subset of data points and objectives simultaneously in all updates, and is particularly suitable in large-scale MTL scenarios.

Convergence analysis and improved complexity. We provide a comprehensive convergence analysis of SDMGrad for stochastic MOO with smooth nonconvex objective functions. For a constant-level regularization parameter λ (which covers the MGDA case), the sample complexities (i.e., the number of samples to achieve an ϵ -accurate Pareto stationary point) of the proposed SDMGrad and SDMGrad-OS improve that of MoCo Fernando et al. (2023) by an order of ϵ^{-2} (see Table 1), without any requirement on the number K of objectives or the number T of iterations. Under an additional bounded function assumption (see Table 2), the sample complexities of SDMGrad and SDMGrad-OS are improved to $\mathcal{O}(\epsilon^{-2})$, which matches the existing best result in Fernando et al. (2023). For an increasing λ , we also show that this convergent point reduces to a stationary point of the linear combination $L_0(\theta)$ of objectives.

Promising empirical performance. We conduct extensive experiments in multi-task supervised learning and reinforcement learning on multiple datasets, and show that SDMGrad can outperform existing state-of-the-art gradient manipulation methods such as MGDA, PCGrad, GradDrop, CAGrad and MoCo, and can strike a better performance balance on different tasks. SDMGrad-OS also exhibits a much better efficiency than SDMGrad in the setting with a large number of tasks due to the efficient objective sampling.

2 Related Works

Multi-task learning. One important application of MOO is MTL, whose target is to learn multiple tasks with possible correlation simultaneously. Due to this capability, MTL has received significant attention in various applications in computer vision, natural language process, robotics and reinforcement learning Hashimoto et al. (2016); Ruder (2017); Zhang & Yang (2021); Vandenhende et al. (2021). A group of studies have focused on how to design better MTL model architectures. For example, Misra et al. (2016); Rosenbaum et al. (2017); Yang et al. (2020) enhance the MTL models by introducing task-specific modules, an attention mechanism, and different activation functions for different tasks, respectively. Another line of research aims to learn a bunch of smaller models of local tasks split from the original problem, which are then aggregated into a single model via knowledge distillation Hinton et al. (2015). Recent several works Wang et al. (2021); Ye et al. (2021) have explored the connection between MTL and gradient-based meta-learning. Fifty et al. (2021) and Meyerson & Miikkulainen (2020) highlight the importance of task grouping and unrelated tasks in MTL, respectively. This paper focuses on a single model by learning multiple tasks simultaneously with novel model-agnostic SDMGrad and SDMGrad-OS methods.

Gradient-based MOO. Various gradient manipulation methods have been developed to learn multiple tasks simultaneously. One popular class of approaches re-weight different objectives based on uncertainty Kendall et al. (2018), gradient norm Chen et al. (2018), and training difficulty Guo et al. (2018). MOO-based approach have received more attention due to the principled designs and training stability. For example, Sener & Koltun (2018) viewed MTL as a MOO problem and proposed MGDA-type method for optimization. A class of approaches have been proposed to address the gradient conflict problem. Among them, Yu et al. (2020a) proposed PCGrad by projecting the gradient direction of each task on the norm plane of other tasks. GradDrop randomly dropped out highly conflicted gradients Chen et al. (2020), and RotoGrad rotated task gradients to alleviate the conflict Javaloy & Valera (2021). Liu et al. (2021) proposed CAGrad by constraining the common direction within a local region around the average gradient. These approaches mainly focus on the deterministic setting. In the stochastic case, Fernando et al. (2023) proposed MoCo as a stochastic counterpart of MGDA, and provided it with a comprehensive convergence and complexity analysis. In this paper, we propose a new stochastic MOO method named SDMGrad, which benefits from a direction-oriented regularization and an improved convergence and complexity performance.

3 Preliminaries

3.1 Pareto Stationarity in MOO

Differently from the single-objective optimization, MOO aims to find points at which all objectives cannot be further optimized. Consider two points θ and θ' . It is claimed that θ dominates θ' if $L_i(\theta) \leq L_i(\theta')$ for all $i \in [K]$ and $L(\theta) \neq L(\theta')$. In the general nonconvex setting, MOO aims to find a Pareto stationary point θ , at which there is no common descent direction for all objectives. In other words, we say θ is a Pareto stationary point if $\text{range}(\nabla L(\theta)) \cap (-\mathbb{R}_{++}^K) = \emptyset$ where \mathbb{R}_{++}^K is the positive orthant cone.

3.2 MGDA and Its Stochastic Variants

Deterministic MGDA. The deterministic MGDA algorithm was first studied by Désidéri (2012), which updates the model parameter θ along a multi-gradient $d = \sum_{i=1}^K w_i^* g_i(\theta) = G(\theta)w^*$, where $G(\theta) =$

$(g_1(\theta), g_2(\theta), \dots, g_K(\theta))$ are the gradients of different objectives, and $w^* := (w_1^*, w_2^*, \dots, w_K^*)^T$ are the weights of different objectives obtained via solving the following problem.

$$w^* \in \arg \min_w \|G(\theta)w\|^2 \quad s.t. \quad w \in \mathcal{W} := \{w \in \mathbb{R}^K \mid \mathbf{1}^T w = 1, w \geq 0\}, \quad (3)$$

where \mathcal{W} is the probability simplex. The deterministic MGDA and its variants such as PCGrad and CAGrad have been well studied, but their stochastic counterparts have not been understood well.

Stochastic MOO algorithms. SMG Liu & Vicente (2021) is the first stochastic variant of MGDA by replacing the full gradient $G(\theta)$ in eq. (3) by its stochastic gradient $G(\theta; \xi)$, and updates the model parameters θ along the direction given by

$$d_\xi = G(\theta; \xi)w_\xi^* \quad s.t. \quad w_\xi^* \in \arg \min_w \|G(\theta; \xi)w\|^2.$$

However, this direct replacement can introduce **biased** multi-gradient estimation, and hence SMG required to increase the batch sizes linearly with the iteration number. To address this limitation, Fernando et al. (2023) proposed MoCo by introducing an additional tracking variable $y_{t,i}$ as the stochastic estimate of the gradient $\nabla L_i(\theta)$, which is iteratively updated via

$$y_{t+1,i} = \Pi_{\mathcal{Y}_i}(y_{t,i} - \beta_t(y_{t,i} - h_{t,i})), i = 1, 2, \dots, K, \quad (4)$$

where β_t is the step size and $\Pi_{\mathcal{Y}_i}$ denotes the projection on a bounded set $\mathcal{Y}_i = \{y \in \mathbb{R}^K \mid \|y\| \leq C_{y,i}\}$ for some constant $C_{y,i}$. Then, MoCo was shown to achieve an asymptotically unbiased multi-gradient, but with a relatively strong assumption that the number T of iterations is much larger than the number K of objectives. Thus, it is important but still challenging to develop provable and easy-to-implement stochastic MOO algorithms with mild assumptions.

4 Our Method

We first provide a new direction-oriented MOO problem, and then introduce a new stochastic MOO algorithm named SDMGrad and its variant SDMGrad-OS with objective sampling.

4.1 Direction-oriented Multi-objective Optimization

MOO generally targets at finding a direction d to maximize the minimum decrease across all objectives via solving the following problem.

$$\max_{d \in \mathbb{R}^m} \min_{i \in [K]} \left\{ \frac{1}{\alpha} (L_i(\theta) - L_i(\theta - \alpha d)) \right\} \approx \max_{d \in \mathbb{R}^m} \min_{i \in [K]} \langle g_i, d \rangle, \quad (5)$$

where the first-order Taylor approximation of L_i is applied at θ with a small stepsize α .

In some scenarios, the target is to not only find the above common descent direction, but also optimize a specific objective that is often a linear combination $L_0(\theta) = \sum_i \tilde{w}_i L_i(\theta)$ for some $\tilde{w} \in \mathcal{W}$ of objectives such as the average loss in MTL. Towards this end, we propose the following multi-objective problem formulation by adding an inner-product regularization $\lambda \langle g_0, d \rangle$ in eq. (5) such that the common descent direction d stays not far away from a target direction $g_0 = \sum_i \tilde{w}_i g_i$.

$$\max_{d \in \mathbb{R}^m} \min_{i \in [K]} \langle g_i, d \rangle - \frac{1}{2} \|d\|^2 + \lambda \langle g_0, d \rangle. \quad (6)$$

In the above eq. (6), the term $-\frac{1}{2}\|d\|^2$ is used to regularize the magnitude of the direction d and the constant λ controls the distance between the update vector d and the target direction g_0 .

Compared to CAGrad. We note that CAGrad also takes a direction-oriented objective but using a different constraint-enforced formulation as follows.

$$\max_{d \in \mathbb{R}^m} \min_{i \in [K]} \langle g_i, d \rangle \quad \text{s.t.} \quad \|d - h_0\| \leq c \|h_0\| \quad (7)$$

where h_0 is the average gradient and $c \in [0, 1)$ is a constant. To optimize eq. (7), CAGrad involves the evaluations of the product $\|h_0\| \|g_w\|$ and the relation $\frac{\|h_0\|}{\|g_w\|}$ with $g_w := \sum_i w_i g_i$, both of which complicate the designs of unbiased stochastic gradient/multi-gradient in the w and θ updates. As a comparison, our formulation in eq. (6), as shown later, admits very simple and provable stochastic algorithmic designs, while still enjoying the direction-oriented benefit as in CAGrad.

To efficiently solve the problem in eq. (6), we then substitute the relation that $\min_{i \in [K]} \langle g_i, d \rangle = \min_{w \in \mathcal{W}} \langle \sum_{i=1}^K g_i w_i, d \rangle = \min_{w \in \mathcal{W}} \langle g_w, d \rangle$ into eq. (6), and obtain an equivalent problem as

$$\max_{d \in \mathbb{R}^m} \min_{w \in \mathcal{W}} \langle g_w + \lambda g_0, d \rangle - \frac{1}{2} \|d\|^2.$$

By switching min and max in the above problem, which does not change the solution due to the concavity in d and the convexity in w , we finally aim to solve $\min_{w \in \mathcal{W}} \max_{d \in \mathbb{R}^m} \langle g_w + \lambda g_0, d \rangle - \frac{1}{2} \|d\|^2$, where the solution to the min problem on w is

$$w_\lambda^* \in \arg \min_{w \in \mathcal{W}} \frac{1}{2} \|g_w + \lambda g_0\|^2, \quad (8)$$

and the solution to the max problem is $d^* = g_{w_\lambda^*} + \lambda g_0$.

Connection with MGDA and GD. It can be seen from eq. (8) that the updating direction d^* reduces to that of MGDA if we set $\lambda = 0$, and is consistent with that of GD for λ large enough. This consistency is also validated empirically in Section 6.1 by varying λ .

4.2 Proposed SDMGrad Algorithm

The natural idea to solve the problem in eq. (8) is to use a simple SGD-type method. However, since the objective in eq. (8) is merely convex w.r.t. w , it can only guarantee the convergence of at least one iterate (not necessarily the last one) to the solution w_λ^* . To ensure the more practical last-iterate convergence, we add a quadratic regularization term in eq. (8), and optimize its smoothed version as

$$w_{\rho, \lambda}^* = \arg \min_{w \in \mathcal{W}} \frac{1}{2} \|g_w + \lambda g_0\|^2 + \frac{\rho}{2} \|w\|^2. \quad (9)$$

Note that $w_{\rho, \lambda}^*$ approximates the original solution w_λ^* up to a small level of ρ . The detailed steps are provided in algorithm 1. At each iteration t , we run S steps of projected SGD with warm-start initialization and with the stochastic gradient that is unbiased by noting that

$$\mathbb{E}_{\xi, \xi'} [G(\theta_t; \xi)^T (G(\theta_t; \xi') w_{t,s} + \lambda G_0(\theta_t; \xi')) + \rho w_{t,s}] = G(\theta_t)^T (G(\theta_t) w_{t,s} + \lambda G_0(\theta_t)) + \rho w_{t,s},$$

where ξ, ξ' are sampled data and $G_0(\theta_t) = G(\theta_t) \tilde{w}$ denote the averaged objective. After obtaining the estimate $w_{t,S}$, SDMGrad updates the model parameters θ_t based on the stochastic counterpart $G(\theta_t; \zeta) w_{t,S} + \lambda G_0(\theta_t; \zeta)$

of the direction $d^* = g_{w_\lambda^*} + \lambda g_0$ with a stepsize of α_t . It can be seen that SDMGrad is simple to implement with efficient SGD type of updates on both w and θ without introducing other auxiliary variables.

Algorithm 1 Stochastic Direction-oriented Multi-objective Gradient descent (SDMGrad)

- 1: **Initialize:** model parameters θ_0 and weights w_0
 - 2: **for** $t = 0, 1, \dots, T - 1$ **do**
 - 3: **for** $s = 0, 1, \dots, S - 1$ **do**
 - 4: Set $w_{t,0} = w_{t-1,S}$ (warm start) and sample data ξ, ξ'
 - 5: $w_{t,s+1} = \Pi_{\mathcal{W}}(w_{t,s} - \beta_t [G(\theta_t; \xi)^T (G(\theta_t; \xi') w_{t,s} + \lambda G_0(\theta_t; \xi')) + \rho w_{t,s}])$
 - 6: **end for**
 - 7: Sample data ζ and $\theta_{t+1} = \theta_t - \alpha_t (G(\theta_t; \zeta) w_{t,S} + \lambda G_0(\theta_t; \zeta))$
 - 8: **end for**
-

4.3 SDMGrad with Objective Sampling (SDMGrad-OS)

Another advantage of SDMGrad is its simple extension via objective sampling to the more practical setting with a large of objectives, e.g., in large-scale MTL. In this setting, we propose SDMGrad-OS by replacing the gradient matrix $G(\theta_t; \xi)$ in Algorithm 1 by a matrix $H(\theta_t; \xi)$ with randomly sampled columns, which takes the form of

$$H(\theta_t; \xi, \mathcal{S}) = (h_1(\theta_t; \xi), h_2(\theta_t; \xi), \dots, h_K(\theta_t; \xi)), \quad (10)$$

where $h_i(\theta_t; \xi) = g_i(\theta_t; \xi)$ with a probability of n/K or 0 otherwise, \mathcal{S} corresponds to the randomness by objective sampling, and n is the expected number of sampled objectives. Then, the stochastic gradient in the w update is adapted to

$$\text{(Gradient on } w) \quad \frac{K^2}{n^2} H(\theta_t; \xi, \mathcal{S})^T (H(\theta_t; \xi', \mathcal{S}') w_{t,s} + \lambda H_0(\theta_t; \xi', \mathcal{S}')) + \rho w_{t,s},$$

where $H_0(\cdot) = H(\cdot) \tilde{w}$. Similarly, the updating direction $d = \frac{K}{n} H(\theta_t; \zeta, \tilde{\mathcal{S}}) w_{t,S} + \frac{K}{n} \lambda H_0(\theta_t; \zeta, \tilde{\mathcal{S}})$. In the practical implementation, we first use *np.random.binomial* to sample a 0-1 sequence s following a Bernoulli distribution with length K and probability n/K , and then compute the gradient $g_i(\theta; \xi)$ of $G(\theta; \xi)$ only if the i^{th} entry of s equals to 1. This sampling strategy greatly speeds up the training with a large number of objectives, as shown by the reinforcement learning experiments in Section 6.3.

5 Main results

5.1 Definitions and Assumptions

We first make some standard definitions and assumptions, as also adopted by existing MOO studies in Liu & Vicente (2021); Fernando et al. (2023); Zhou et al. (2022). Since we focus on the practical setting where the objectives are nonconvex, algorithms are often expected to find an ϵ -accurate Pareto stationary point, as defined below.

Definition 1. We say $\theta \in \mathbb{R}^m$ is an ϵ -accurate Pareto stationary point if $\mathbb{E}[\min_{w \in \mathcal{W}} \|g_w(\theta)\|^2] \leq \epsilon$ where \mathcal{W} is the probability simplex.

The following assumption imposes the Lipschitz continuity on the objectives and their gradients.

Assumption 1. For every task $i \in [K]$, $L_i(\theta)$ is l_i -Lipschitz continuous and $\nabla L_i(\theta)$ is $l_{i,1}$ -Lipschitz continuous for any $\theta \in \mathbb{R}^m$.

We next make an assumption on the bias and variance of the stochastic gradient $g_i(\theta; \xi)$.

Assumption 2. For every task $i \in [K]$, the gradient $g_i(\theta; \xi)$ is the unbiased estimate of $g_i(\theta)$. Moreover, the gradient variance is bounded by $\mathbb{E}_\xi[\|g_i(\theta; \xi) - g_i(\theta)\|^2] \leq \sigma_i^2$.

Assumption 3. Assume there exists a constant $C_g > 0$ such that $\|G(\theta)\| \leq C_g$.

The bounded gradient condition in Assumption 3 is necessary to ensure the boundedness of the multi-gradient estimation error, as also adopted by Zhou et al. (2022); Fernando et al. (2023).

5.2 Convergence Analysis with Nonconvex Objectives

We first characterize the bias for estimating the multi-gradient $G(\theta_t)w_{t,\lambda}^* + \lambda G_0(\theta_t)$, where $w_{t,\lambda}^* \in \arg \min_{w \in \mathcal{W}} \frac{1}{2} \|g_w + \lambda g_0\|^2$ at the t -th iteration.

Proposition 1. Suppose Assumptions 1-3 are satisfied. Let $C_1 = \mathcal{O}(K^2 + \lambda^2 K^2)$. Then we have

$$\begin{aligned} & \mathbb{E}[\|\mathbb{E}[G(\theta_t; \zeta)w_{t,S} + \lambda G_0(\theta_t; \zeta)] - G(\theta_t)w_{t,\lambda}^* - \lambda G_0(\theta_t)\|^2 | \theta_t] \\ & \leq 8C_g^2(1 - 2\beta_t\rho)^S + \frac{3\beta_t C_g^2 C_1}{\rho} + \rho. \end{aligned} \quad (11)$$

Proposition 1 shows that the error bound contains an exponentially decaying term $\mathcal{O}((1 - 2\beta_t\rho)^S)$, and two small terms $\frac{3\beta_t C_g^2 C_1}{\rho} + \rho$ that are controllable with sufficiently small stepsize β_t and smoothing constant ρ . Based on this important property, we obtain the following general convergence result.

Theorem 1 (SDMGrad). Suppose Assumption 1-3 are satisfied. Set $\alpha_t = \alpha = \Theta((1 + \lambda)^{-1}K^{-\frac{1}{2}}T^{-\frac{1}{2}})$, $\beta_t = \beta = \Theta((1 + \lambda^2)K^{-1}T^{-2})$, and $\rho = \Theta(K(1 + \lambda^2)T^{-1})$. Furthermore, if we choose $S = \Theta(\frac{1}{(1 + \lambda^2)^2}T^3)$, then the outputs of the proposed SDMGrad algorithm satisfies

$$\frac{1}{T} \sum_{t=0}^{T-1} \mathbb{E}[\|G(\theta_t)w_{t,\lambda}^* + \lambda G_0(\theta_t)\|^2] = \mathcal{O}((1 + \lambda^2)K^{\frac{1}{2}}T^{-\frac{1}{2}}). \quad (12)$$

Theorem 1 establishes a general convergence guarantee for SDMGrad along the gradient direction $d^* = g_{w_\lambda^*} + \lambda g_0$. Building on Theorem 1, we next show that with different choices of the regularization parameter λ , two types of convergence results can be obtained in the following two corollaries. Define $w_t^* \in \arg \min_{w \in \mathcal{W}} \frac{1}{2} \|G(\theta_t)w\|^2$ at the t -th iteration.

Corollary 1 (Constant λ). Under the same setting as in Theorem 1, choosing a constant-level $\lambda > 0$, we have $\frac{1}{T} \sum_{t=0}^{T-1} \mathbb{E}[\|G(\theta_t)w_t^*\|^2] = \mathcal{O}(K^{\frac{1}{2}}T^{-\frac{1}{2}})$. To achieve an ϵ -accurate Pareto stationary point, each objective requires $\mathcal{O}(K^4\epsilon^{-8})$ samples in ξ (ξ') and $\mathcal{O}(K\epsilon^{-2})$ samples in ζ , respectively.

Note that Corollary 1 covers the MGDA case where $\lambda = 0$. In this setting, the sampling complexity $\mathcal{O}(\epsilon^{-8})$ improves that of MoCo Fernando et al. (2023) by an order of ϵ^{-2} , without any requirement on K and T .

Corollary 2 (Increasing λ). *Under the same setting as in Theorem 1 and choosing $\lambda = \Theta(T^{\frac{1}{4}})$, we have $\frac{1}{T} \sum_{t=0}^{T-1} \mathbb{E}[\|G_0(\theta_t)\|^2] = \mathcal{O}(K^{\frac{1}{2}}T^{-\frac{1}{2}})$. To achieve an ϵ -accurate stationary point, each objective requires $\mathcal{O}(K^3\epsilon^{-6})$ samples in ξ (ξ') and $\mathcal{O}(K\epsilon^{-2})$ samples in ζ , respectively.*

Corollary 2 analyzes the case with an increasing $\lambda = \Theta(T^{\frac{1}{4}})$, we show that SDMGrad converges to a stationary point of the objective $L_0(\theta) = \sum_i \tilde{w}_i L_i(\theta)$ with an improved sample complexity. This justifies the flexibility of our framework that the λ can balance the worst local improvement of individual objectives and the target objective $L_0(\theta)$.

Convergence under objective sampling. Now we provide a convergence analysis for SDMGrad-OS.

Theorem 2 (SDMGrad-OS). *Suppose Assumption 1-3 are satisfied. Define $\gamma = \frac{K}{n}$ and set parameters $\alpha_t = \alpha = \Theta((1 + \lambda^2)^{-\frac{1}{2}}\gamma^{-\frac{1}{2}}K^{-\frac{1}{2}}T^{-\frac{1}{2}})$, $\beta_t = \beta = \Theta((1 + \lambda^2)^2K^{-1}T^{-2})$, $\rho = \Theta((1 + \lambda^2)\gamma KT^{-1})$, and $S = \Theta((1 + \lambda^2)^{-2}\gamma^{-1}T^3)$. Then, the iterates of the proposed SDMGrad-OS algorithm satisfy*

$$\frac{1}{T} \sum_{t=0}^{T-1} \mathbb{E}[\|G(\theta_t)w_t^*\|^2] = \mathcal{O}(K^{\frac{1}{2}}\gamma^{\frac{1}{2}}T^{-\frac{1}{2}}).$$

Theorem 2 establishes the convergence guarantee for our SDMGrad-OS algorithm, which achieves a per-objective sample complexity of $\mathcal{O}(\epsilon^{-8})$ comparable to that of SDMGrad, but with a much better efficiency due to the objective sampling, as also validated by the empirical comparison in Table 6.

5.3 Convergence under Bounded Function Assumption

In this section, we analyze the convergence of SDMGrad and SDMGrad-OS under an additional assumption that the function values $L_i(\theta), i \in [K]$ are bounded, as also studied by Fernando et al. (2023); Zhou et al. (2022).

5.4 Convergence under Bounded Function Assumption

In this section, we analyze the convergence of SDMGrad and SDMGrad-OS under an additional assumption that the function values $L_i(\theta), i \in [K]$ are bounded, as also studied by Fernando et al. (2023); Zhou et al. (2022).

Theorem 3. *Suppose Assumption 1-3 are satisfied and there exists a constant $F > 0$ such that $\forall t \in [T], \|L(\theta_t)\| \leq F$. Set $\alpha = \Theta((1 + \lambda^2)^{-\frac{1}{2}}K^{-\frac{1}{2}}T^{-\frac{1}{2}})$ and $\beta = \Theta((1 + \lambda^2)^{-\frac{1}{2}}K^{-1}T^{-1})$. The iterates of the proposed SDMGrad algorithm satisfy*

$$\frac{1}{T} \sum_{t=0}^{T-1} E[\|G(\theta_t)w_{t,S} + \lambda G_0(\theta_t)\|^2] = \mathcal{O}((1 + \lambda)^2 K^{\frac{1}{2}} T^{-\frac{1}{2}}).$$

Corollary 3 (Constant λ). *Under the same setting as in Theorem 3 and choosing a constant-level $\lambda > 0$, we have $\frac{1}{T} \sum_{t=0}^{T-1} \mathbb{E}[\|G(\theta_t)w_t^*\|^2] = \mathcal{O}(K^{\frac{1}{2}}T^{-\frac{1}{2}})$. To achieve an ϵ -accurate Pareto stationary point, each objective requires $\mathcal{O}(K\epsilon^{-2})$ samples in ξ (ξ') and $\mathcal{O}(K\epsilon^{-2})$ samples in ζ , respectively.*

A corollary similar to Corollary 2 with an increasing λ can also be obtained in this setting but is omitted due to space limitation.

Convergence under objective sampling. We next analyze the convergence of SDMGrad-OS.

Theorem 4. Suppose Assumption 1-3 are satisfied and there exists a constant $F > 0$ such that $\forall t \in [T]$, $\|\mathbf{L}(\theta_t)\| \leq F$. Set $\gamma = \frac{K}{n}$, $\alpha = \Theta\left(\sqrt{\frac{1}{KT\gamma(1+\lambda^2)}}\right)$ and $\beta = \Theta((1 + \lambda^2)^{-\frac{1}{2}}K^{-1}T^{-1}\gamma^{-1})$. Then by choosing a constant λ , we have

$$\frac{1}{T} \sum_{t=0}^{T-1} \mathbb{E}[\|G(\theta_t)w_t^*\|^2] = \mathcal{O}(K^{\frac{1}{2}}\gamma^{\frac{1}{2}}T^{-\frac{1}{2}}).$$

6 Experiments

In this section, we first verify that the performance of our proposed method is consistent with the principle of our direction-oriented formulation under different regularization constant λ . Then we demonstrate the effectiveness of our proposed methods under a couple of multi-task supervised learning and reinforcement settings. The experimental details and more empirical results such as the two-objective toy example and training curves can be found in the Appendix A.

6.1 Consistency Verification

We conduct the experiment on the multi-task classification dataset Multi-Fashion+MNIST Lin et al. (2019). Each image contained in this dataset is constructed by overlaying two images randomly sampled from MNIST LeCun et al. (1998) and Fashion-MNIST Xiao et al. (2017) respectively. We adopt shrunked Lenet Lecun et al. (1998) as the shared base-encoder and a task-specific linear classification head for each task. We report the training losses obtained from different methods over 3 independent runs in Fig. 1. As illustrated, the performance of SDMGrad with large λ is similar to GD, and the performance when λ is small resembles MGDA. With properly tuned λ , lower average training loss can be obtained. Generally, the results confirm the consistency of our formulation with the direction-oriented principle.



Figure 1: Consistency verification on Multi-Fashion+MNIST dataset.

6.2 Supervised Learning

For the supervised learning setting, we evaluate the performance on the Cityscapes Cordts et al. (2016) and NYU-v2 Nathan Silberman & Fergus (2012) datasets. The former dataset involves 2 pixel-wise tasks: 7-class semantic segmentation and depth estimation, and the latter one involves 3 pixel-wise tasks: 13-class semantic segmentation, depth estimation and surface normal estimation. Following the experimental setup of Liu et al. (2021), we embed a MTL method MTAN Liu et al. (2019) into our SDMGrad method, which builds on SegNet Badrinarayanan et al. (2017) and is empowered by a task-specific attention mechanism. We compare SDMGrad with vanilla MTAN Liu et al. (2019), Cross-Stitch Misra et al. (2016), PCGrad Yu et al. (2020a), GradDrop Chen et al. (2020), CAGrad Liu et al. (2021) and MoCo Fernando et al. (2023). Following Maninis et al. (2019); Liu et al. (2021); Fernando et al. (2023), we compute the average per-task performance drop versus the single-task baseline b to assess method m : $\Delta m = \frac{1}{K} \sum_{k=1}^K (-1)^{l_k} (M_{m,k} - M_{b,k}) / M_{b,k}$ where

Method	Segmentation		Depth		$\Delta m\% \downarrow$
	(Higher Better)		(Lower Better)		
	mIoU	Pix Acc	Abs Err	Rel Err	
Independent	74.01	93.16	0.0125	27.77	
Cross-Stitch Misra et al. (2016)	73.08	92.79	0.0165	118.5	90.02
MTAN Liu et al. (2019)	75.18	93.49	0.0155	46.77	22.60
MGDA Sener & Koltun (2018)	68.84	91.54	0.0309	33.50	44.14
PCGrad Yu et al. (2020a)	75.13	93.48	0.0154	42.07	18.29
GradDrop Chen et al. (2020)	75.27	93.53	0.0157	47.54	23.73
CAGrad Liu et al. (2021)	75.16	93.48	0.0141	37.60	11.64
MoCo Fernando et al. (2023)	75.42	93.55	0.0149	34.19	9.90
SDMGrad ($\lambda = 0.7$)	75.49	93.58	0.0142	37.33	11.46
SDMGrad ($\lambda = 0.3$)	75.00	93.43	0.0135	35.35	8.39

Table 3: Multi-task supervised learning on Cityscapes dataset.

K is the number of tasks, and $l_k = 1$ if the evaluation metric M_k on task k prefers a higher value and 0 otherwise.

We search the hyperparameter $\lambda \in \{0.1, 0.2, \dots, 1.0\}$ for our SDMGrad method and report the results with the best per-task performance drop Δm and with the best average training loss. Results are shown in Table 3 and Table 4. Each experiment is repeated 3 times with different random seeds and the average is reported. It can be seen that our proposed method is able to obtain better or comparable results than the baselines, and in addition, can strike a better performance balance on multiple tasks than other baselines. For example, although MGDA achieves better results on Surface Normal, it performs the worst on both Segmentation and Depth. As a comparison, our SDMGrad method can achieve the best or the second best results on all tasks.

6.3 Reinforcement Learning

For the reinforcement learning setting, we evaluate the performance on the MT10 and MT50 benchmarks, which include 10 and 50 robot manipulation tasks under the Meta-World environment Yu et al. (2020b), respectively. Following the experiment setup in Liu et al. (2021), we adopt Soft Actor-Critic (SAC) Haarnoja et al. (2018) as the underlying training algorithm. We compare SDMGrad with Multi-task SAC Yu et al. (2020b), Multi-headed SAC Yu et al. (2020b), Multi-task SAC + Task Encoder Yu et al. (2020b), PCGrad Yu et al. (2020a), CAGrad Liu et al. (2021) and MoCo Fernando et al. (2023). We search $\lambda \in \{0.1, 0.2, \dots, 1.0\}$ for MT10 and $\lambda \in \{0.2, 0.4, \dots, 1.0\}$ for MT50. As shown by the results in Table 5, SDMGrad achieves a better or comparable performance than the comparison baselines.

We also validate the efficiency of the proposed objective sampling strategy in Table 6. We choose the task sampling size $n = 4$ for MT10 benchmark and $n = 8$ for MT50 benchmark. We report the success rate and the training time (in seconds) per episode of both SDMGrad and SDMGrad-OS. As shown in Table 6, our SDMGrad-OS with objective sampling achieves approximately 1.4x speedup on MT10 and 2.5x speedup, while achieving a success rate comparable to that of SDMGrad.

Method	Segmentation		Depth		Surface Normal					$\Delta m\% \downarrow$
	(Higher Better)		(Lower Better)		Angle Distance (Lower Better)		Within t° (Higher Better)			
	mIoU	Pix Acc	Abs Err	Rel Err	Mean	Median	11.25	22.5	30	
Independent	38.30	63.76	0.6754	0.2780	25.01	19.21	30.14	57.20	69.15	
Cross-Stitch Misra et al. (2016)	37.42	63.51	0.5487	0.2188	28.85	24.52	22.75	46.58	59.56	6.96
MTAN Liu et al. (2019)	39.29	65.33	0.5493	0.2263	28.15	23.96	22.09	47.50	61.08	5.59
MGDA Sener & Koltun (2018)	30.47	59.90	0.6070	0.2555	24.88	19.45	29.18	56.88	69.36	1.38
PCGrad Yu et al. (2020a)	38.06	64.64	0.5550	0.2325	27.41	22.80	23.86	49.83	63.14	3.97
GradDrop Chen et al. (2020)	39.39	65.12	0.5455	0.2279	27.48	22.96	23.38	49.44	62.87	3.58
CAGrad Liu et al. (2021)	39.79	65.49	0.5486	0.2250	26.31	21.58	25.61	52.36	65.58	0.20
MoCo Fernando et al. (2023)	40.30	66.07	0.5575	0.2135	26.67	21.83	25.61	51.78	64.85	0.16
SDMGrad ($\lambda = 0.8$)	40.88	66.33	0.5330	0.2183	26.14	21.40	25.92	52.73	65.94	-1.22
SDMGrad ($\lambda = 0.3$)	39.03	65.35	0.5416*	0.2155*	25.44*	20.43*	27.32*	54.84*	67.81*	-2.58

Table 4: Multi-task supervised learning on NYU-v2 dataset. * : the second best result.

Method	Metaworld MT10	Metaworld MT50
	success (mean \pm stderr)	success (mean \pm stderr)
Multi-task SAC Yu et al. (2020b)	0.49 \pm 0.073	0.36 \pm 0.013
Multi-task SAC + Task Encoder Yu et al. (2020b)	0.54 \pm 0.047	0.40 \pm 0.024
Multi-headed SAC Yu et al. (2020b)	0.61 \pm 0.036	0.45 \pm 0.064
PCGrad Yu et al. (2020a)	0.72 \pm 0.022	0.50 \pm 0.017
CAGrad Liu et al. (2021)	0.83 \pm 0.045	0.52 \pm 0.023
MoCo Fernando et al. (2023)	0.75 \pm 0.050	–
SDMGrad (Ours)	0.84 \pm 0.049	0.52 \pm 0.029
One SAC agent per task (upper bound)	0.90 \pm 0.032	0.74 \pm 0.041

Table 5: Multi-task reinforcement learning on Metaworld benchmarks.

Method	Metaworld MT10		Metaworld MT50	
	success (mean \pm stderr)	time	success (mean \pm stderr)	time
SDMGrad	0.84 \pm 0.049	13.3	0.52 \pm 0.029	42.8
SDMGrad-OS	0.82 \pm 0.040	9.7	0.49 \pm 0.033	16.8

Table 6: Validation on the efficiency of the proposed objective sampling.

7 Conclusion

In this paper, we propose a new and flexible direction-oriented multi-objective problem, as well as two simple and efficient MOO algorithms named SDMGrad and SDMGrad-OS. We establish the convergence guarantee

for both algorithms in various settings. Extensive experiments validate the promise of our methods. We anticipate that our new problem formulation and the proposed algorithms can be applied in other learning applications with multiple measures, and the analysis can be of independent interest in analyzing other stochastic MOO algorithms.

References

- Vijay Badrinarayanan, Alex Kendall, and Roberto Cipolla. Segnet: A deep convolutional encoder-decoder architecture for image segmentation. *IEEE transactions on pattern analysis and machine intelligence*, 39(12):2481–2495, 2017.
- Jonathan M Borwein. A very complicated proof of the minimax theorem. *Minimax Theory and its Applications*, 1(1):21–27, 2016.
- Zhao Chen, Vijay Badrinarayanan, Chen-Yu Lee, and Andrew Rabinovich. Gradnorm: Gradient normalization for adaptive loss balancing in deep multitask networks. In *International conference on machine learning*, pp. 794–803. PMLR, 2018.
- Zhao Chen, Jiquan Ngiam, Yanping Huang, Thang Luong, Henrik Kretzschmar, Yuning Chai, and Dragomir Anguelov. Just pick a sign: Optimizing deep multitask models with gradient sign dropout. *Advances in Neural Information Processing Systems*, 33:2039–2050, 2020.
- Marius Cordts, Mohamed Omran, Sebastian Ramos, Timo Rehfeld, Markus Enzweiler, Rodrigo Benenson, Uwe Franke, Stefan Roth, and Bernt Schiele. The cityscapes dataset for semantic urban scene understanding. In *Proc. of the IEEE Conference on Computer Vision and Pattern Recognition (CVPR)*, 2016.
- Jean-Antoine Désidéri. Multiple-gradient descent algorithm (mgda) for multiobjective optimization. *Comptes Rendus Mathématique*, 350(5-6):313–318, 2012.
- Heshan Devaka Fernando, Han Shen, Miao Liu, Subhajit Chaudhury, Keerthiram Murugesan, and Tianyi Chen. Mitigating gradient bias in multi-objective learning: A provably convergent approach. In *The Eleventh International Conference on Learning Representations*, 2023.
- Chris Fifty, Ehsan Amid, Zhe Zhao, Tianhe Yu, Rohan Anil, and Chelsea Finn. Efficiently identifying task groupings for multi-task learning. *Advances in Neural Information Processing Systems (NeurIPS)*, 34: 27503–27516, 2021.
- Michelle Guo, Albert Haque, De-An Huang, Serena Yeung, and Li Fei-Fei. Dynamic task prioritization for multitask learning. In *Proceedings of the European conference on computer vision (ECCV)*, pp. 270–287, 2018.
- Tuomas Haarnoja, Aurick Zhou, Pieter Abbeel, and Sergey Levine. Soft actor-critic: Off-policy maximum entropy deep reinforcement learning with a stochastic actor. In *International conference on machine learning*, pp. 1861–1870. PMLR, 2018.
- Kazuma Hashimoto, Caiming Xiong, Yoshimasa Tsuruoka, and Richard Socher. A joint many-task model: Growing a neural network for multiple nlp tasks. *arXiv preprint arXiv:1611.01587*, 2016.

- Geoffrey Hinton, Oriol Vinyals, and Jeff Dean. Distilling the knowledge in a neural network. *arXiv preprint arXiv:1503.02531*, 2015.
- Xinyu Huang, Peng Wang, Xinjing Cheng, Dingfu Zhou, Qichuan Geng, and Ruigang Yang. The apolloscape open dataset for autonomous driving and its application. *IEEE transactions on pattern analysis and machine intelligence*, 42(10):2702–2719, 2019.
- Adrián Javaloy and Isabel Valera. Rotograd: Gradient homogenization in multitask learning. *arXiv preprint arXiv:2103.02631*, 2021.
- Alex Kendall, Yarin Gal, and Roberto Cipolla. Multi-task learning using uncertainty to weigh losses for scene geometry and semantics. In *Proceedings of the IEEE conference on computer vision and pattern recognition*, pp. 7482–7491, 2018.
- Y. Lecun, L. Bottou, Y. Bengio, and P. Haffner. Gradient-based learning applied to document recognition. *Proceedings of the IEEE*, 86(11):2278–2324, 1998. doi: 10.1109/5.726791.
- Yann LeCun, Léon Bottou, Yoshua Bengio, and Patrick Haffner. Gradient-based learning applied to document recognition. *Proceedings of the IEEE*, 86(11):2278–2324, 1998.
- Xi Lin, Hui-Ling Zhen, Zhenhua Li, Qing-Fu Zhang, and Sam Kwong. Pareto multi-task learning. In H. Wallach, H. Larochelle, A. Beygelzimer, F. d'Alché-Buc, E. Fox, and R. Garnett (eds.), *Advances in Neural Information Processing Systems*, volume 32. Curran Associates, Inc., 2019. URL https://proceedings.neurips.cc/paper_files/paper/2019/file/685bfbde03eb646c27ed565881917c71c-Paper.pdf.
- Bo Liu, Xingchao Liu, Xiaojie Jin, Peter Stone, and Qiang Liu. Conflict-averse gradient descent for multi-task learning. *Advances in Neural Information Processing Systems*, 34:18878–18890, 2021.
- Shikun Liu, Edward Johns, and Andrew J Davison. End-to-end multi-task learning with attention. In *Proceedings of the IEEE/CVF conference on computer vision and pattern recognition*, pp. 1871–1880, 2019.
- Suyun Liu and Luis Nunes Vicente. The stochastic multi-gradient algorithm for multi-objective optimization and its application to supervised machine learning. *Annals of Operations Research*, pp. 1–30, 2021.
- Jiaqi Ma, Zhe Zhao, Xinyang Yi, Jilin Chen, Lichan Hong, and Ed H Chi. Modeling task relationships in multi-task learning with multi-gate mixture-of-experts. In *Proceedings of the 24th ACM SIGKDD international conference on knowledge discovery & data mining*, pp. 1930–1939, 2018.
- Kevis-Kokitsi Maninis, Ilija Radosavovic, and Iasonas Kokkinos. Attentive single-tasking of multiple tasks. In *Proceedings of the IEEE/CVF Conference on Computer Vision and Pattern Recognition*, pp. 1851–1860, 2019.
- Elliot Meyerson and Risto Miikkulainen. The traveling observer model: Multi-task learning through spatial variable embeddings. *arXiv preprint arXiv:2010.02354*, 2020.

- Ishan Misra, Abhinav Shrivastava, Abhinav Gupta, and Martial Hebert. Cross-stitch networks for multi-task learning. In *Proceedings of the IEEE conference on computer vision and pattern recognition*, pp. 3994–4003, 2016.
- Pushmeet Kohli Nathan Silberman, Derek Hoiem and Rob Fergus. Indoor segmentation and support inference from rgb-d images. In *ECCV*, 2012.
- Clemens Rosenbaum, Tim Klinger, and Matthew Riemer. Routing networks: Adaptive selection of non-linear functions for multi-task learning. *arXiv preprint arXiv:1711.01239*, 2017.
- Sebastian Ruder. An overview of multi-task learning in deep neural networks. *arXiv preprint arXiv:1706.05098*, 2017.
- Ozan Sener and Vladlen Koltun. Multi-task learning as multi-objective optimization. *Advances in neural information processing systems*, 31, 2018.
- Shagun Sodhani and Amy Zhang. Mtrl - multi task rl algorithms. Github, 2021. URL <https://github.com/facebookresearch/mtrl>.
- Philip S Thomas, Joelle Pineau, Romain Laroche, et al. Multi-objective spibb: Seldonian offline policy improvement with safety constraints in finite mdps. *Advances in Neural Information Processing Systems*, 34:2004–2017, 2021.
- Simon Vandenhende, Stamatios Georgoulis, Wouter Van Gansbeke, Marc Proesmans, Dengxin Dai, and Luc Van Gool. Multi-task learning for dense prediction tasks: A survey. *IEEE transactions on pattern analysis and machine intelligence*, 44(7):3614–3633, 2021.
- Haoxiang Wang, Han Zhao, and Bo Li. Bridging multi-task learning and meta-learning: Towards efficient training and effective adaptation. In *International Conference on Machine Learning (ICML)*, pp. 10991–11002. PMLR, 2021.
- Han Xiao, Kashif Rasul, and Roland Vollgraf. Fashion-mnist: a novel image dataset for benchmarking machine learning algorithms. *arXiv preprint arXiv:1708.07747*, 2017.
- Ruihan Yang, Huazhe Xu, Yi Wu, and Xiaolong Wang. Multi-task reinforcement learning with soft modularization. *Advances in Neural Information Processing Systems*, 33:4767–4777, 2020.
- Feiyang Ye, Baijiong Lin, Zhixiong Yue, Pengxin Guo, Qiao Xiao, and Yu Zhang. Multi-objective meta learning. *Advances in Neural Information Processing Systems (NeurIPS)*, 34:21338–21351, 2021.
- Junyu You, William Ampomah, and Qian Sun. Development and application of a machine learning based multi-objective optimization workflow for co2-eor projects. *Fuel*, 264:116758, 2020.
- Tianhe Yu, Saurabh Kumar, Abhishek Gupta, Sergey Levine, Karol Hausman, and Chelsea Finn. Gradient surgery for multi-task learning. *Advances in Neural Information Processing Systems*, 33:5824–5836, 2020a.
- Tianhe Yu, Deirdre Quillen, Zhanpeng He, Ryan Julian, Karol Hausman, Chelsea Finn, and Sergey Levine. Meta-world: A benchmark and evaluation for multi-task and meta reinforcement learning. In *Conference on robot learning*, pp. 1094–1100. PMLR, 2020b.

Yu Zhang and Qiang Yang. A survey on multi-task learning. *IEEE Transactions on Knowledge and Data Engineering*, 34(12):5586–5609, 2021.

Shiji Zhou, Wenpeng Zhang, Jiyan Jiang, Wenliang Zhong, Jinjie Gu, and Wenwu Zhu. On the convergence of stochastic multi-objective gradient manipulation and beyond. *Advances in Neural Information Processing Systems*, 35:38103–38115, 2022.

Supplementary Materials

A Experiments

Practical implementation of projected gradient descent. Consider the objective g , w lies in probability simplex while g_w and g_0 are related to the gradient of each task. w and g may in different scales, thus lead to potential numerical problem during training process. To alleviate the issue, we can rescale the objective by a constant without changing the optimal solution. For projection operation, we choose Euclidean projection to probability simplex instead of softmax, which is used in MoCo Fernando et al. (2023).

A.1 Toy Example

To demonstrate our proposed method can achieve better or comparable performance under stochastic settings, we provide an empirical study on the two-objective toy example used in CAGrad Liu et al. (2021). The two objectives $L_1(x)$ and $L_2(x)$ shown in Fig.2 are defined on $x = (x_1, x_2)^\top \in \mathbb{R}^2$,

$$\begin{aligned}L_1(x) &= f_1(x)g_1(x) + f_2(x)h_1(x) \\L_2(x) &= f_1(x)g_2(x) + f_2(x)h_2(x),\end{aligned}$$

where the functions are given by

$$\begin{aligned}f_1(x) &= \max(\tanh(0.5x_2), 0) \\f_2(x) &= \max(\tanh(-0.5x_2), 0) \\g_1(x) &= \log\left(\max(|0.5(-x_1 - 7) - \tanh(-x_2)|, 0.000005)\right) + 6 \\g_2(x) &= \log\left(\max(|0.5(-x_1 + 3) - \tanh(-x_2) + 2|, 0.000005)\right) + 6 \\h_1(x) &= ((-x_1 + 7)^2 + 0.1(-x_1 - 8)^2)/10 - 20 \\h_2(x) &= ((-x_1 - 7)^2 + 0.1(-x_1 - 8)^2)/10 - 20.\end{aligned}$$

We choose 3 initializations

$$x_0 \in \{(-8.5, 7.5), (-8.5, 5), (9, 9)\}$$

for different methods and visualize the optimization trajectories in Fig.2. The starting point of every trajectory in Fig.2d-2h is given by the \bullet symbol, and the color of every trajectory changes gradually from red to yellow. The gray line illustrates the Pareto front, and the \star symbol denotes the global optimum. To simulate the stochastic setting, we add zero-mean Gaussian noise to the gradient of each objective for all the methods except MGDA. We adopt Adam optimizer with learning rate of 0.002 and 70000 iterations for each run. As shown, GD can get stuck due to the dominant gradient of a specific objective, which stops progressing towards the Pareto front. PCGrad and CAGrad can also fail to converge to the Pareto front in certain circumstances.

A.2 Consistency Verification

The Multi-Fashion+MNISTLin et al. (2019) includes images constructed from FashionMNISTXiao et al. (2017) and MNISTLeCun et al. (1998). First, select one image from each dataset randomly, then transform

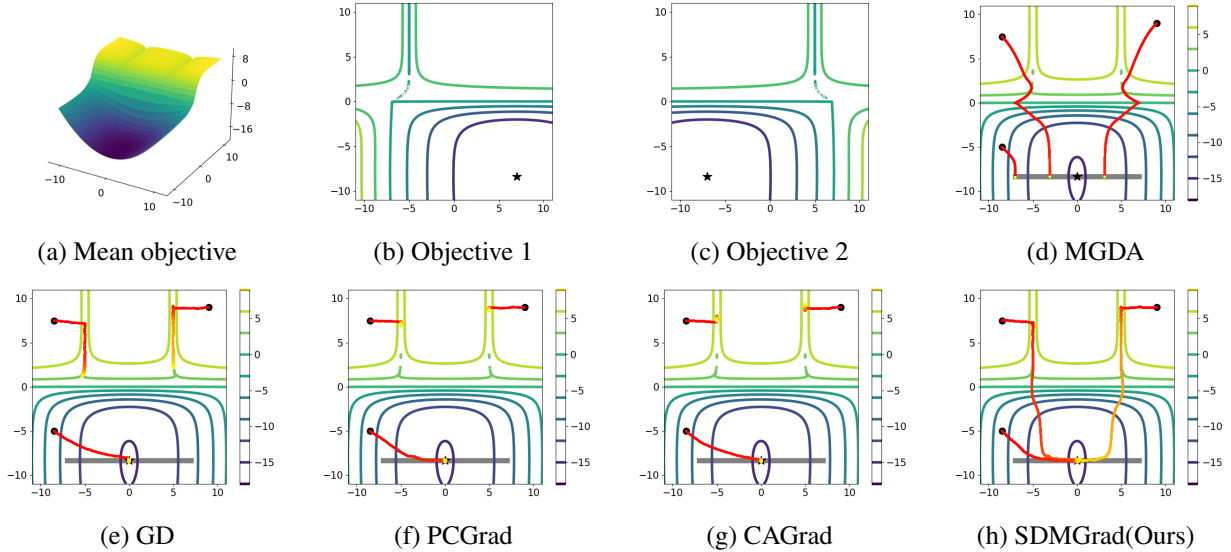


Figure 2: A two-objective toy example

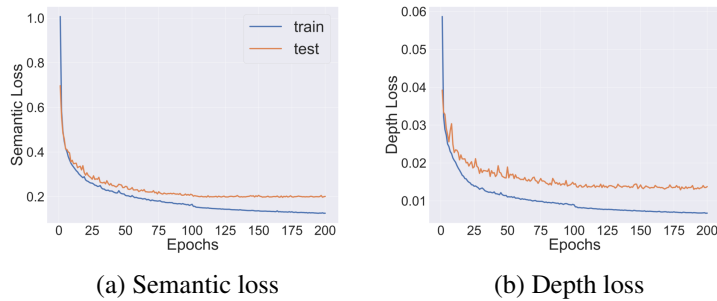


Figure 3: Training and test loss curves for Cityscapes tasks

the two images into a single image with one put in the top-left corner and the other in bottom-right corner. The dataset contains 120000 training images and 20000 test images. We use SGD optimizer with learning rate 0.001 and train for 100 epochs with batch size 256. We use multi-step scheduler with scale factor 0.1 to decay learning rate every 15 epochs. The projected gradient descent is performed with learning rate of 10 and momentum of 0.5 and 20 gradient descent steps are applied.

A.3 Supervised Learning

Following CAGradLiu et al. (2021) and MoCoFernando et al. (2023), we train our method for 200 epochs, using Adam optimizer with learning rate 0.0001 for the first 100 epochs and 0.00005 for the rest. The batch size for Cityscapes and NYU-v2 are 8 and 2 respectively. We compute the averaged test performance over the last 10 epochs as final performance measure. The inner projected gradient descent is performed with learning rate of 10 and momentum of 0.5 and 20 gradient descent steps are applied. We provide training and test loss curves for multiple tasks contained in both datasets in Fig.3 and Fig.4.

We also compare our proposed method with CAGradLiu et al. (2021) when the best performance drop is

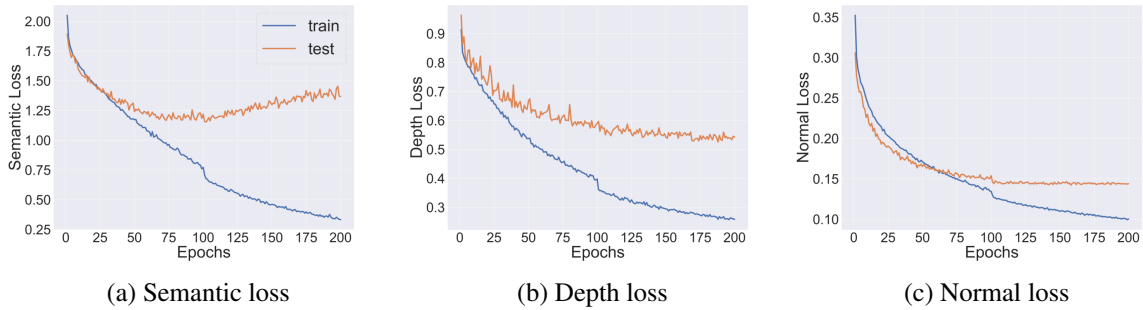


Figure 4: Training and test loss curves for NYU-v2 tasks

achieved in Table 7 and Table 8.

Method	Segmentation		Depth		$\Delta m\% \downarrow$
	(Higher Better)		(Lower Better)		
	mIoU	Pix Acc	Abs Err	Rel Err	
Independent	74.01	93.16	0.0125	27.77	
CAGrad ($c = 0.8$)	74.95	93.50	0.0143	36.05	10.74
SDMGrad ($\lambda = 0.3$)	75.00	93.43	0.0135	35.35	8.39

Table 7: Multi-task supervised learning on Cityscapes dataset with best performance drop

Method	Segmentation		Depth		Surface Normal					$\Delta m\% \downarrow$
	(Higher Better)		(Lower Better)		Angle Distance		Within t°			
	mIoU	Pix Acc	Abs Err	Rel Err	(Lower Better)		(Higher Better)			
					Mean	Median	11.25	22.5	30	
Independent	38.30	63.76	0.6754	0.2780	25.01	19.21	30.14	57.20	69.15	
CAGrad ($c = 0.8$)	39.18	64.97	0.5379	0.2229	25.42	20.47	27.37	54.73	67.73	-2.29
SDMGrad ($\lambda = 0.3$)	39.03	65.35	0.5416	0.2155	25.44	20.43	27.32	54.84	67.81	-2.58

Table 8: Multi-task supervised learning on NYU-v2 dataset with best performance drop

A.4 Reinforcement Learning

Following CAGradLiu et al. (2021) and MoCoFernando et al. (2023), we conduct the experiments based on MTRL codebaseSodhani & Zhang (2021). We train our method for 2 million steps with batch size of 1280. The inner projected gradient descent is performed with learning rate of 25 for MT10 benchmark and 50 for MT50 benchmark and 20 gradient descent steps are applied. The method is evaluated once every 10000 steps

and the best average test performance over 5 random seeds over the entire training process is reported. We search $\lambda \in \{0.1, 0.2, \dots, 1.0\}$ for MT10 benchmark and $\lambda \in \{0.2, 0.4, \dots, 1.0\}$ for MT50 benchmark. For our objective sampling strategy, the number of sampled objectives is a random variable obeying binomial distribution whose expectation is n . To compare with CAGradLiu et al. (2021), we choose $n = 4$ for MT10 benchmark and $n = 8$ for MT50 benchmark.

B Notations for Technical Proofs

In this part, we first summarize all the notations that we used in this paper in order to help readers understand. First, in multi-task learning (MTL), we have $K \geq 2$ different tasks and each of them has the loss function $L_i(\theta)$. The goal of the MTL is to minimize the average loss over K tasks. g_i denotes the gradient of task i and g_0 denotes the average gradient. $w = (w_1, \dots, w_K)^T \in \mathbb{R}^K$ and \mathcal{W} denotes the probability simplex. Other useful notations are listed as below:

$$\begin{aligned}
\theta^* &= \arg \min_{\theta \in \mathbb{R}^m} \left\{ L_0(\theta) \triangleq \frac{1}{K} \sum_{i=1}^K L_i(\theta) \right\}, \quad g_0 = G_0(\theta) = G(\theta)\tilde{w} \\
g_w &= \sum_i w_i g_i \quad \text{s.t.} \quad \mathcal{W} = \{w : \sum_i w_i = 1 \text{ and } w_i \geq 0\} \\
w_\lambda^* &= \arg \min_{w \in \mathcal{W}} \frac{1}{2} \|g_w + \lambda g_0\|^2, \quad w^* = \arg \min_{w \in \mathcal{W}} \frac{1}{2} \|g_w\|^2, \quad w_t^* = \arg \min_{w \in \mathcal{W}} \frac{1}{2} \|G(\theta_t)w\|^2 \\
w_{t,\lambda}^* &= \arg \min_{w \in \mathcal{W}} \frac{1}{2} \|G(\theta_t)w + \lambda G(\theta_t)\tilde{w}\|^2, \quad w_{\rho,\lambda}^* = \arg \min_{w \in \mathcal{W}} \frac{1}{2} \|g_w + \lambda g_0\|^2 + \frac{\rho}{2} \|w\|^2 \\
w_{t,\rho,\lambda}^* &= \arg \min_{w \in \mathcal{W}} \frac{1}{2} \|G(\theta_t) + \lambda G(\theta_t)\tilde{w}\|^2 + \frac{\rho}{2} \|w\|^2.
\end{aligned} \tag{13}$$

C Detailed proofs for convergence analysis with nonconvex Objectives

We now provide some auxiliary lemmas for proving Proposition 1 and Theorem 1

Lemma 1. *Let d^* be the solution of*

$$\max_{d \in \mathbb{R}^m} \min_{i \in [K]} \langle g_i, d \rangle - \frac{1}{2} \|d\|^2 + \lambda \langle g_0, d \rangle,$$

then we have

$$d^* = g_{w_\lambda^*} + \lambda g_0.$$

In addition, w_λ^ is the solution of*

$$\min_{w \in \mathcal{W}} \frac{1}{2} \|g_w + \lambda g_0\|^2.$$

Proof. First, it can be seen that

$$\max_{d \in \mathbb{R}^m} \min_{i \in [K]} \langle g_i, d \rangle - \frac{1}{2} \|d\|^2 + \lambda \langle g_0, d \rangle$$

$$\begin{aligned}
&= \max_{d \in \mathbb{R}^m} \min_{w \in \mathcal{W}} \left\langle \sum_i w_i g_i, d \right\rangle - \frac{1}{2} \|d\|^2 + \lambda \langle g_0, d \rangle \\
&= \max_{d \in \mathbb{R}^m} \min_{w \in \mathcal{W}} g_w^T d - \frac{1}{2} \|d\|^2 + \lambda \langle g_0, d \rangle.
\end{aligned} \tag{14}$$

Noting that the problem is concave w.r.t. d and convex w.r.t w and using the Von Neumann-Fan minimax theorem Borwein (2016), we can exchange the min and max problems without changing the solution. Then, we can solve the following equivalent problem.

$$\min_{w \in \mathcal{W}} \max_{d \in \mathbb{R}^m} g_w^T d - \frac{1}{2} \|d\|^2 + \lambda \langle g_0, d \rangle \tag{15}$$

Then by fixing w , we have $d^* = g_w + \lambda g_0$. Substituting this solution to the eq. (15) and rearranging the equation, we turn to solve the following problem.

$$\min_{w \in \mathcal{W}} \frac{1}{2} \|g_w + \lambda g_0\|^2.$$

Let w_λ^* be the solution of the above problem, and hence the final updating direction $d^* = g_{w_\lambda^*} + \lambda g_0$. Then, the proof is complete. \square

Lemma 2. *Suppose Assumption 1-2 are satisfied. According to the definition of $G_0(\theta)$ in eq. (13), we have the following inequalities,*

$$\|G_0(\theta)\| \leq C_g, \quad \mathbb{E}[\|G_0(\theta; \xi) - G_0(\theta)\|^2] \leq K\sigma_0^2.$$

Proof. Based on the definitions, we have

$$\|G_0(\theta)\| = \|G(\theta)\tilde{w}\| \leq C_g,$$

where the inequality follows from the fact that $\|\tilde{w}\| \leq 1$ and Assumption 3. Then, we have

$$\mathbb{E}_\xi[\|G_0(\theta; \xi) - G_0(\theta)\|^2] \leq \mathbb{E}_\xi[\|G(\theta; \xi) - G(\theta)\|^2] \leq K\sigma_0^2$$

where $\sigma_0^2 = \max_i \sigma_i^2$ and the proof is complete. \square

Lemma 3. *Suppose Assumptions 1-3 are satisfied. Let $w_{\rho, \lambda}^* = \arg \min_{w \in \mathcal{W}} \frac{1}{2} \|g_w + \lambda g_0\|^2 + \frac{\rho}{2} \|w\|^2$. Then we have*

$$\mathbb{E}[\|w_S - w_{\rho, \lambda}^*\|^2] \leq 4(1 - 2\beta_t \rho)^S + \frac{3\beta_t C_1}{2\rho},$$

where $C_1 = 4(K\sigma_0^2 + C_g^2)^2 + 4\lambda^2(K\sigma_0^2 + C_g^2)^2 + \rho^2 = \mathcal{O}(K^2 + \lambda^2 K^2)$.

Proof. From Algorithm 1, the unbiased stochastic gradient is given by

$$\nabla w_s = G(\theta; \xi)^T (G(\theta; \xi') w_s + \lambda G_0(\theta; \xi')) + \rho w_s.$$

Thus, we can obtain that

$$\|w_{s+1} - w_{\rho, \lambda}^*\| = \|\Pi_{\mathcal{W}}(w_s - \beta_t \nabla w_s) - w_{\rho, \lambda}^*\|$$

$$\begin{aligned}
& \stackrel{(i)}{=} \|\Pi_{\mathcal{W}}(w_s - \beta_t \nabla w_s) - \Pi_{\mathcal{W}}(w_{\rho, \lambda}^*)\| \\
& \stackrel{(ii)}{\leq} \|w_s - \beta_t \nabla w_s - w_{\rho, \lambda}^*\|
\end{aligned} \tag{16}$$

where (i) is due to the fact that $w_{\rho, \lambda}^*$ is in the projection set and (ii) follows from the non-expansive property of projection onto convex set. Then, we have

$$\begin{aligned}
\|w_{s+1} - w_{\rho, \lambda}^*\|^2 & \leq \|w_s - w_{\rho, \lambda}^*\|^2 + \beta_t^2 \|\nabla w_s\|^2 - 2\beta_t \langle w_s - w_{\rho, \lambda}^*, \nabla w_s \rangle \\
& \stackrel{(i)}{\leq} (1 - 2\beta_t \rho) \|w_s - w_{\rho, \lambda}^*\|^2 + \beta_t^2 \|G(\theta; \xi)^T (G(\theta; \xi') w_s + \lambda G_0(\theta; \xi')) + \rho w_s\|^2 \\
& \stackrel{(ii)}{\leq} (1 - 2\beta_t \rho) \|w_s - w_{\rho, \lambda}^*\|^2 + 3\beta_t^2 \underbrace{\|G(\theta; \xi)^T G(\theta; \xi')\|^2}_{\textcircled{1}} \\
& \quad + \lambda^2 \underbrace{\|G(\theta; \xi)^T G_0(\theta; \xi')\|^2}_{\textcircled{2}} + \rho^2,
\end{aligned} \tag{17}$$

where (i) follows from strong convexity and (ii) follows from Young's inequality. Now we bound $\textcircled{1}$ and $\textcircled{2}$, respectively:

$$\begin{aligned}
\mathbb{E}[\textcircled{1}] & = \mathbb{E}[\|(G(\theta; \xi)^T - G(\theta)^T + G(\theta)^T)(G(\theta; \xi') - G(\theta) + G(\theta))\|^2] \\
& = \mathbb{E}[\|(G(\theta; \xi)^T - G(\theta)^T)(G(\theta; \xi') - G(\theta)) + (G(\theta; \xi)^T - G(\theta)^T)G(\theta) \\
& \quad + G(\theta)^T(G(\theta; \xi') - G(\theta)) + G(\theta)^T G(\theta)\|^2] \\
& \stackrel{(i)}{\leq} 4\mathbb{E}[\|G(\theta; \xi)^T - G(\theta)^T\|^2 \|G(\theta; \xi') - G(\theta)\|^2] + 4\mathbb{E}[\|G(\theta; \xi)^T - G(\theta)^T\|^2 \|G(\theta)\|^2] \\
& \quad + 4\mathbb{E}[\|G(\theta)^T\|^2 \|G(\theta; \xi') - G(\theta)\|^2] + 4\mathbb{E}[\|G(\theta)^T G(\theta)\|^2] \\
& \stackrel{(ii)}{\leq} 4K^2 \sigma_0^4 + 8K \sigma_0^2 C_g^2 + 4C_g^4 = 4(K \sigma_0^2 + C_g^2)^2,
\end{aligned} \tag{18}$$

where (i) follows from Young's inequality, (ii) follows from Assumption 2-3, and σ_0 is defined in Lemma 2. Then we bound $\textcircled{2}$ using similar steps as

$$\begin{aligned}
\mathbb{E}[\textcircled{2}] & = \mathbb{E}[\|(G(\theta; \xi)^T - G(\theta)^T)(G_0(\theta; \xi') - G_0(\theta)) + (G(\theta; \xi)^T - G(\theta)^T)G_0(\theta) \\
& \quad + G(\theta)^T(G_0(\theta; \xi') - G_0(\theta)) + G(\theta)^T G_0(\theta)\|^2] \\
& \stackrel{(i)}{\leq} 4\mathbb{E}[\|G(\theta; \xi)^T - G(\theta)^T\|^2 \|G_0(\theta; \xi') - G_0(\theta)\|^2] + 4\mathbb{E}[\|G(\theta; \xi)^T - G(\theta)^T\|^2 \|G_0(\theta)\|^2] \\
& \quad + 4\mathbb{E}[\|G(\theta)^T\|^2 \|G_0(\theta; \xi') - G_0(\theta)\|^2] + 4\mathbb{E}[\|G(\theta)^T G_0(\theta)\|^2] \\
& \stackrel{(ii)}{\leq} 4K^2 \sigma_0^4 + 8K \sigma_0^2 C_g^2 + 4C_g^4 = 4(K \sigma_0^2 + C_g^2)^2,
\end{aligned} \tag{19}$$

where (i) follows from Young's inequality and (ii) follows from Assumption 3 and Lemma 2. Then taking expectation on both sides of eq. (17) and substituting eq. (19) and eq. (18) into eq. (17), we have

$$\begin{aligned}
\mathbb{E}[\|w_{s+1} - w_{\rho, \lambda}^*\|^2] & \leq (1 - 2\beta_t \rho) \mathbb{E}[\|w_s - w_{\rho, \lambda}^*\|^2] \\
& \quad + 3\beta_t^2 \underbrace{(4(K \sigma_0^2 + C_g^2)^2 + 4\lambda^2 (K \sigma_0^2 + C_g^2)^2 + \rho^2)}_{C_1}
\end{aligned}$$

$$=(1 - 2\beta_t\rho)\mathbb{E}[\|w_s - w_{\rho,\lambda}^*\|^2] + 3\beta_t^2C_1.$$

Then, telescoping over s from 0 to $S - 1$, yields

$$\begin{aligned}\mathbb{E}[\|w_S - w_{\rho,\lambda}^*\|^2] &\leq (1 - 2\beta_t\rho)^S \mathbb{E}[\|w_0 - w_{\rho,\lambda}^*\|^2] + \frac{3\beta_t C_1}{2\rho} \\ &\leq 4(1 - 2\beta_t\rho)^S + \frac{3\beta_t C_1}{2\rho}.\end{aligned}\tag{20}$$

where the last inequality follows from Young's inequality and the fact that each weight $\|w\| \leq 1$. The proof is complete. \square

C.1 Proof of Proposition 1

Now we show the bias of our estimator is bounded.

Proof. Based on the definitions of $G(\cdot)$ and $G_0(\cdot)$, we have

$$\begin{aligned}\mathbb{E}[\|\mathbb{E}[G(\theta_t;\zeta)w_{t,S} + \lambda G_0(\theta_t;\zeta)] - G(\theta_t)w_{t,\lambda}^* - \lambda G_0(\theta_t)\|^2|\theta_t] & \\ = \mathbb{E}[\|G(\theta_t)w_{t,S} - G(\theta_t)w_{t,\lambda}^*\|^2] & \\ = \mathbb{E}[\|G(\theta_t)w_{t,S} - G(\theta_t)w_{t,\rho,\lambda}^* + G(\theta_t)w_{t,\rho,\lambda}^* - G(\theta_t)w_{t,\lambda}^*\|^2] & \\ \stackrel{(i)}{\leq} 2\mathbb{E}[\|G(\theta_t)w_{t,S} - G(\theta_t)w_{t,\rho,\lambda}^*\|^2] + 2\mathbb{E}[\|G(\theta_t)w_{t,\rho,\lambda}^* - G(\theta_t)w_{t,\lambda}^*\|^2] & \\ \stackrel{(ii)}{\leq} 2C_g^2\mathbb{E}[\|w_{t,S} - w_{t,\rho,\lambda}^*\|^2] + 2\mathbb{E}[\|G(\theta_t)w_{t,\rho,\lambda}^* + \lambda G_0(\theta_t)\|^2 + \|G(\theta_t)w_{t,\lambda}^* + \lambda G_0(\theta_t)\|^2] & \\ \quad - 2\mathbb{E}\langle G(\theta_t)w_{t,\rho,\lambda}^* + \lambda G_0(\theta_t), G(\theta_t)w_{t,\lambda}^* + \lambda G_0(\theta_t)\rangle & \\ \stackrel{(iii)}{\leq} 2C_g^2\mathbb{E}[\|w_{t,S} - w_{t,\rho,\lambda}^*\|^2] + 2\mathbb{E}[\|G(\theta_t)w_{t,\rho,\lambda}^* + \lambda G_0(\theta_t)\|^2 - \|G(\theta_t)w_{t,\lambda}^* + \lambda G_0(\theta_t)\|^2] & \\ \stackrel{(iv)}{\leq} 8C_g^2(1 - 2\beta_t\rho)^S + \frac{3\beta_t C_g^2 C_1}{\rho} + \rho &\end{aligned}\tag{21}$$

where (i) follows from Young's inequality, (ii) follows from Assumption 3, (iii) follows from optimality condition that

$$\langle w, G(\theta_t)^T(G(\theta_t)w_{t,\lambda}^* + \lambda G_0(\theta_t)) \rangle \geq \langle w_{t,\lambda}^*, G(\theta_t)^T(G(\theta_t)w_{t,\lambda}^* + \lambda G_0(\theta_t)) \rangle\tag{22}$$

for any $w \in \mathcal{W}$, and (iv) follows from the optimality that

$$\|G(\theta_t)w_{t,\rho,\lambda}^* + \lambda G_0(\theta_t)\|^2 + \frac{\rho}{2}\|w_{t,\rho,\lambda}^*\|^2 \leq \|G(\theta_t)w_{t,\lambda}^* + \lambda G_0(\theta_t)\|^2 + \frac{\rho}{2}\|w_{t,\lambda}^*\|^2$$

and $\|w_{t,\lambda}^*\| \leq 1$. Then, the proof is complete. \square

C.2 Proof of Theorem 1

Theorem 5 (Restatement of Theorem 1). *Suppose Assumption 1-3 are satisfied. Set $\alpha_t = \alpha = \Theta((1 + \lambda)^{-1}K^{-\frac{1}{2}}T^{-\frac{1}{2}})$, $\beta_t = \beta = \Theta((1 + \lambda^2)K^{-1}T^{-2})$, and $\rho = \Theta(K(1 + \lambda^2)T^{-1})$. Furthermore, if we choose $S = \Theta(\frac{1}{(1 + \lambda^2)^2}T^3)$, then the outputs of the proposed SDMGrad algorithm satisfies*

$$\frac{1}{T} \sum_{t=0}^{T-1} \mathbb{E}[\|G(\theta_t)w_{t,\lambda}^* + \lambda G_0(\theta_t)\|^2] = \mathcal{O}((1 + \lambda^2)K^{\frac{1}{2}}T^{-\frac{1}{2}}).$$

Proof. Recall that $d = G(\theta_t; \zeta)w_{t,S} + \lambda G_0(\theta_t; \zeta)$. According to Assumption 1, we have for any i ,

$$L_i(\theta_{t+1}) + \lambda L_0(\theta_{t+1}) \leq L_i(\theta_t) + \lambda L_0(\theta_t) + \alpha_t \langle g_i(\theta_t) + \lambda G_0(\theta_t), -d \rangle + \frac{l'_{i,1} \alpha_t^2}{2} \|d\|^2. \quad (23)$$

where $l'_{i,1} = l_{i,1} + \lambda \max_i l_{i,1} = \Theta(1 + \lambda)$. Then we bound the second and third terms separately on the right-hand side (RHS). First, for the second term, conditioning on θ_t and taking expectation, we have

$$\begin{aligned} & \mathbb{E}[\langle g_i(\theta_t) + \lambda G_0(\theta_t), -G(\theta_t; \zeta)w_{t,S} - \lambda G_0(\theta_t; \zeta) \rangle] \\ &= \mathbb{E}[\langle g_i(\theta_t) + \lambda G_0(\theta_t), -G(\theta_t)w_{t,S} - \lambda G_0(\theta_t) \rangle] \\ &= \mathbb{E}[\langle g_i(\theta_t) + \lambda G_0(\theta_t), G(\theta_t)w_{t,\lambda}^* - G(\theta_t)w_{t,S} \rangle - \langle g_i(\theta_t) + \lambda G_0(\theta_t), G(\theta_t)w_{t,\lambda}^* + \lambda G_0(\theta_t) \rangle] \\ &\stackrel{(i)}{\leq} \mathbb{E}[(l_i + \lambda C_g) \|G(\theta_t)w_{t,\lambda}^* - G(\theta_t)w_{t,S}\|] - \|G(\theta_t)w_{t,\lambda}^* + \lambda G_0(\theta_t)\|^2 \\ &= \mathbb{E}[(l_i + \lambda C_g) \|G(\theta_t)w_{t,\lambda}^* - G(\theta_t)w_{t,\rho,\lambda}^* + G(\theta_t)w_{t,\rho,\lambda}^* - G(\theta_t)w_{t,S}\|] \\ &\quad - \|G(\theta_t)w_{t,\lambda}^* + \lambda G_0(\theta_t)\|^2 \\ &\stackrel{(ii)}{\leq} (l_i + \lambda C_g) (\|G(\theta_t)w_{t,\lambda}^* - G(\theta_t)w_{t,\rho,\lambda}^*\| + C_g \mathbb{E}[\|w_{t,S} - w_{t,\rho,\lambda}^*\|]) \\ &\quad - \|G(\theta_t)w_{t,\lambda}^* + \lambda G_0(\theta_t)\|^2 \\ &\stackrel{(iii)}{\leq} (l_i + \lambda C_g) \left(\sqrt{\frac{\rho}{2}} + C_g \mathbb{E}[\|w_{t,S} - w_{t,\rho,\lambda}^*\|] \right) - \|G(\theta_t)w_{t,\lambda}^* + \lambda G_0(\theta_t)\|^2, \end{aligned} \quad (24)$$

where (i) follows from Cauchy-schwarz inequality and eq. (22), (ii) follows from Assumption 3 and (iii) follows from eq. (21). Then for the third term,

$$\begin{aligned} \mathbb{E}[\|d\|^2] &= \mathbb{E}[\|G(\theta_t; \zeta)w_{t,S} + \lambda G_0(\theta_t; \zeta)\|^2] \\ &= \mathbb{E}[\|G(\theta_t; \zeta)w_{t,S} - G(\theta_t)w_{t,S} + G(\theta_t)w_{t,S} + \lambda G_0(\theta_t; \zeta) - \lambda G_0(\theta_t) + \lambda G_0(\theta_t)\|^2] \\ &\stackrel{(i)}{\leq} 4\mathbb{E}[\|G(\theta_t; \zeta) - G(\theta_t)\|^2] + 4\mathbb{E}[\|G(\theta_t)\|^2] + 4\lambda^2 \mathbb{E}[\|G_0(\theta_t; \zeta) - G_0(\theta_t)\|^2] \\ &\quad + 4\lambda^2 \mathbb{E}[\|G_0(\theta_t)\|^2] \\ &\stackrel{(ii)}{\leq} \underbrace{4K\sigma_0^2 + 4C_g^2 + 4\lambda^2 K\sigma_0^2 + 4\lambda^2 C_g^2}_{C_2} \end{aligned} \quad (25)$$

where (i) follows from Young's inequality, (ii) follows from Assumption 3 and Lemma 2. Note that $C_2 = \mathcal{O}(K + K\lambda^2)$. Then taking expectation on eq. (23), substituting eq. (24) and eq. (25) into it, and unconditioning on θ_t , we have

$$\begin{aligned} & \mathbb{E}[L_i(\theta_{t+1}) + \lambda L_0(\theta_{t+1})] \\ &\leq \mathbb{E}[L_i(\theta_t) + \lambda L_0(\theta_t)] + \alpha_t \mathbb{E}[\langle g_i(\theta_t) + \lambda G_0(\theta_t), -d \rangle] + \frac{l'_{i,1} \alpha_t^2}{2} \mathbb{E}[\|d\|^2] \\ &\leq \mathbb{E}[L_i(\theta_t) + \lambda L_0(\theta_t)] + \alpha_t (l_i + \lambda C_g) \left(\sqrt{\frac{\rho}{2}} + C_g \mathbb{E}[\|w_{t,S} - w_{t,\rho,\lambda}^*\|] \right) \\ &\quad - \alpha_t \mathbb{E}[\|G(\theta_t)w_{t,\lambda}^* + \lambda G_0(\theta_t)\|^2] + \frac{l'_{i,1} \alpha_t^2}{2} C_2 \end{aligned} \quad (26)$$

Then, choosing $\alpha_t = \alpha$, $\beta_t = \beta$ and rearranging the above inequality, we have

$$\begin{aligned} \alpha \mathbb{E}[\|G(\theta_t)w_{t,\lambda}^* + \lambda G_0(\theta_t)\|^2] &\leq \mathbb{E}[L_i(\theta_t) + \lambda L_0(\theta_t) - L_i(\theta_{t+1}) - \lambda L_0(\theta_{t+1})] \\ &\quad + \alpha(l_i + \lambda C_g) \left(\sqrt{\frac{\rho}{2}} + C_g \mathbb{E}[\|w_{t,S} - w_{t,\rho,\lambda}^*\|] \right) + \frac{l'_{i,1}\alpha^2}{2} C_2. \end{aligned}$$

Telescoping over $t \in [T]$ in the above inequality yields

$$\begin{aligned} &\frac{1}{T} \sum_{t=0}^{T-1} \mathbb{E}[\|G(\theta_t)w_{t,\lambda}^* + \lambda G_0(\theta_t)\|^2] \\ &\leq \frac{1}{\alpha T} \mathbb{E}[L_i(\theta_0) - \inf L_i(\theta) + \lambda(L_0(\theta_0) - \inf L_0(\theta))] + \frac{l'_{i,1}\alpha}{2} C_2 \\ &\quad + (l_i + \lambda C_g) \frac{1}{T} \sum_{t=0}^{T-1} \left(\sqrt{\frac{\rho}{2}} + C_g \mathbb{E}[\|w_{t,S} - w_{t,\rho,\lambda}^*\|] \right) \\ &\leq \frac{1}{\alpha T} \mathbb{E}[L_i(\theta_0) - \inf L_i(\theta) + \lambda(L_0(\theta_0) - \inf L_0(\theta))] + \frac{l'_{i,1}\alpha}{2} C_2 \\ &\quad + (l_i + \lambda C_g) \left(\sqrt{\frac{\rho}{2}} + C_g \sqrt{4(1 - 2\beta\rho)^S + \frac{3\beta C_1}{2\rho}} \right), \end{aligned}$$

where the last inequality follows from eq. (20) in Lemma 3. If we choose $\alpha = \Theta((1 + \lambda)^{-1} K^{-\frac{1}{2}} T^{-\frac{1}{2}})$, $\beta = \Theta((1 + \lambda^2) K^{-1} T^{-2})$, $\rho = \Theta(K(1 + \lambda^2) T^{-1})$ and $S = \Theta((1 + \lambda^2)^{-2} T^3)$, we have

$$\frac{1}{T} \sum_{t=0}^{T-1} \mathbb{E}[\|G(\theta_t)w_{t,\lambda}^* + \lambda G_0(\theta_t)\|^2] = \mathcal{O}((1 + \lambda^2) K^{\frac{1}{2}} T^{-\frac{1}{2}}).$$

The proof is complete. \square

C.3 Proof of Corollary 1

Proof. Since $\lambda > 0$ and $G_0(\theta_t) = G(\theta_t)\tilde{w}$, we have

$$\mathbb{E}[\|G(\theta_t)w_{t,\lambda}^* + \lambda G_0(\theta_t)\|^2] = (1 + \lambda)^2 \mathbb{E}[\|G(\theta_t)w'\|^2] \geq (1 + \lambda)^2 \mathbb{E}[\|G(\theta_t)w_t^*\|^2]$$

where $w' = \frac{1}{1+\lambda}(w_{1,t,\lambda}^* + \lambda\tilde{w}_1, w_{2,t,\lambda}^* + \lambda\tilde{w}_2, \dots, w_{K,t,\lambda}^* + \lambda\tilde{w}_K)^T$ such that $w' \in \mathcal{W}$. According to parameter selection in Theorem 1 and by choosing a constant λ , we have

$$\frac{1}{T} \sum_{t=0}^{T-1} \mathbb{E}[\|G(\theta_t)w_t^*\|^2] = \mathcal{O}(K^{\frac{1}{2}} T^{-\frac{1}{2}}). \quad (27)$$

To achieve an ϵ -accurate Pareto stationary point, it requires $T = \mathcal{O}(K\epsilon^{-2})$ and each objective requires $\mathcal{O}(K^4\epsilon^{-8})$ samples in ξ (ξ') and $\mathcal{O}(K\epsilon^{-2})$ samples in ζ , respectively. \square

C.4 Proof of Corollary 2

Proof. According to the inequality $\|a + b - b\|^2 \leq 2\|a + b\|^2 + 2\|b\|^2$, we have

$$\begin{aligned}\lambda^2 \|G_0(\theta_t)\|^2 &\leq 2\|G(\theta_t)w_{t,\lambda}^* + \lambda G_0(\theta_t)\|^2 + 2\|G(\theta_t)w_t\|^2 \\ &\leq 2\|G(\theta_t)w_{t,\lambda}^* + \lambda G_0(\theta_t)\|^2 + 2C_g^2\end{aligned}$$

where the last inequality follows from Assumption 3. Then we take the expectation on the above inequality and sum up it over $t \in [T]$ such that

$$\begin{aligned}\frac{1}{T} \sum_{t=0}^{T-1} \mathbb{E}[\|G_0(\theta_t)\|^2] &\leq \frac{2}{\lambda^2 T} \sum_{t=0}^{T-1} \mathbb{E}[\|G(\theta_t)w_{t,\lambda}^* + \lambda G_0(\theta_t)\|^2] + \frac{C_g^2}{\lambda^2} \\ &\leq \mathcal{O}((\lambda^{-2} + 1)K^{\frac{1}{2}}T^{-\frac{1}{2}} + \lambda^{-2}),\end{aligned}$$

where the last inequality follows from Theorem 1. If we choose $\lambda = \Theta(T^{\frac{1}{4}})$, then we have

$$\frac{1}{T} \sum_{t=0}^{T-1} \mathbb{E}[\|G_0(\theta_t)\|^2] \leq \mathcal{O}(K^{\frac{1}{2}}T^{-\frac{1}{2}}).$$

To achieve an ϵ -accurate Pareto stationary point, it requires $T = \mathcal{O}(K\epsilon^{-2})$ and each objective requires $\mathcal{O}(K^3\epsilon^{-6})$ samples in ξ (ξ') and $\mathcal{O}(K\epsilon^{-2})$ samples in ζ , respectively. \square

C.5 Proof of Theorem 2

Now we provide the convergence analysis with nonconvex objectives.

Lemma 4. *Suppose Assumptions 1-3 are satisfied. Let $w_{\rho,\lambda}^* = \arg \min_{w \in \mathcal{W}} \frac{1}{2}\|g_w + \lambda g_0\|^2 + \frac{\rho}{2}\|w\|^2$. Then we have the following inequality.*

$$\mathbb{E}[\|w_S - w_{\rho,\lambda}^*\|^2] \leq 4(1 - 2\beta_t\rho)^S + \frac{3\beta_t C'_1}{2\rho},$$

where $C'_1 = 4\gamma^4(n\sigma_0^2 + C_g^2)^2 + 4\lambda^2\gamma^4(n\sigma_0^2 + C_g^2)^2 + \rho^2$.

Proof. Under the objective sampling, the unbiased stochastic gradient is given by

$$\nabla w'_s = \gamma^2 H(\theta_t; \xi, \mathcal{S})^T (H(\theta_t; \xi', \mathcal{S}')w_{t,s} + \lambda H_0(\theta_t; \xi', \mathcal{S}')) + \rho w_{t,s}$$

Then taking similar steps as in eq. (16), we can obtain that

$$\|w_{s+1} - w_{\rho,\lambda}^*\| \leq \|w_s - \beta_t \nabla w'_s - w_{\rho,\lambda}^*\|$$

Further, following the same steps as in Lemma 3 we have

$$\mathbb{E}[\|w_{s+1} - w_{\rho,\lambda}^*\|^2] \leq (1 - 2\beta_t\rho)\mathbb{E}[\|w_s - w_{\rho,\lambda}^*\|^2] + 3\beta_t^2 C'_1, \quad (28)$$

where $C'_1 = 4\gamma^4(n\sigma_0^2 + C_g^2)^2 + 4\lambda^2\gamma^4(n\sigma_0^2 + C_g^2)^2 + \rho^2$. Then telescoping eq. (28) over s from 0 to $S - 1$ yields

$$\mathbb{E}[\|w_S - w_{\rho,\lambda}^*\|^2] \leq 4(1 - 2\beta_t\rho)^S + \frac{3\beta_t C'_1}{2\rho}. \quad (29)$$

The proof is complete. \square

Theorem 6 (Restatement of Theorem 2). *Suppose Assumption 1-3 are satisfied. Set $\gamma = \frac{K}{n}$, $\alpha_t = \alpha = \Theta((1 + \lambda^2)^{-\frac{1}{2}}\gamma^{-\frac{1}{2}}K^{-\frac{1}{2}}T^{-\frac{1}{2}})$, $\beta_t = \beta = \Theta((1 + \lambda^2)^2K^{-1}T^{-2})$, $\rho = \Theta((1 + \lambda^2)\gamma KT^{-1})$ and $S = \Theta((1 + \lambda^2)^{-2}\gamma^{-1}T^3)$. Then by choosing a constant λ , the iterates of the proposed SDMGrad-OS algorithm satisfy*

$$\frac{1}{T} \sum_{t=0}^{T-1} \mathbb{E}[\|G(\theta_t)w_t^*\|^2] = \mathcal{O}(K^{\frac{1}{2}}\gamma^{\frac{1}{2}}T^{-\frac{1}{2}}).$$

Proof. Recall that updating direction for θ_t is $d' = \frac{K}{n}H(\theta_t; \zeta, \tilde{S})w_{t,S} + \frac{K}{n}\lambda H_0(\theta_t; \zeta, \tilde{S})$. Similarly, we have

$$L_i(\theta_{t+1}) + \lambda L_0(\theta_{t+1}) \leq L_i(\theta_t) + \lambda L_0(\theta_t) + \alpha_t \langle g_i(\theta_t) + \lambda G_0(\theta_t), -d' \rangle + \frac{l'_{i,1}\alpha_t^2}{2} \|d'\|^2. \quad (30)$$

Then for the inner product term on the RHS of eq. (30), conditioning on θ_t and taking expectation, we have

$$\begin{aligned} \mathbb{E}[\langle g_i(\theta_t) + \lambda G_0(\theta_t), -d' \rangle] &= \mathbb{E}[\langle g_i(\theta_t) + \lambda G_0(\theta_t), -G(\theta_t)w_{t,S} - \lambda G_0(\theta_t) \rangle] \\ &\leq (l_i + \lambda C_g) \left(\sqrt{\frac{\rho}{2}} + C_g \mathbb{E}[\|w_{t,S} - w_{t,\rho,\lambda}^*\|] \right) - \|G(\theta_t)w_{t,\lambda}^* + \lambda G_0(\theta_t)\|^2, \end{aligned} \quad (31)$$

where the last inequality follows from eq. (24). Then following the same step as in eq. (25), we can bound the last term on the RHS of eq. (30) as

$$\mathbb{E}[\|d'\|^2] \leq \underbrace{4\gamma^2(1 + \lambda^2)(n\sigma_0^2 + C_g^2)}_{C'_2}. \quad (32)$$

Then taking expectation on eq. (30), substitute eq. (31) and eq. (32) into it and unconditioning on θ_t , we have

$$\begin{aligned} \mathbb{E}[L_i(\theta_{t+1}) + \lambda L_0(\theta_{t+1})] &\leq \mathbb{E}[L_i(\theta_t) + \lambda L_0(\theta_t)] + \alpha_t (l_i + \lambda C_g) \left(\sqrt{\frac{\rho}{2}} + C_g \mathbb{E}[\|w_{t,S} - w_{t,\rho,\lambda}^*\|] \right) \\ &\quad - \alpha_t \mathbb{E}[\|G(\theta_t)w_{t,\lambda}^* + \lambda G_0(\theta_t)\|^2] + \frac{l'_{i,1}\alpha_t^2}{2} C'_2 \\ &\leq \mathbb{E}[L_i(\theta_t) + \lambda L_0(\theta_t)] + \alpha_t (l_i + \lambda C_g) \left(\sqrt{\frac{\rho}{2}} + C_g \sqrt{4(1 - 2\beta_t\rho)^S + \frac{3\beta_t C'_1}{2\rho}} \right) \\ &\quad - \alpha_t \mathbb{E}[\|G(\theta_t)w_{t,\lambda}^* + \lambda G_0(\theta_t)\|^2] + \frac{l'_{i,1}\alpha_t^2}{2} C'_2 \end{aligned}$$

Then choosing $\alpha_t = \alpha$, $\beta_t = \beta$, telescoping the above inequality over $t \in [T]$, and rearrange the terms, we have

$$\begin{aligned} \frac{1}{T} \sum_{t=0}^{T-1} \mathbb{E}[\|G(\theta_t)w_{t,\lambda}^* + \lambda G_0(\theta_t)\|^2] &\leq \frac{1}{\alpha T} \mathbb{E}[L_i(\theta_0) - \inf L_i(\theta) + \lambda(L_0(\theta_0) - \inf L_0(\theta))] + \frac{l'_{i,1}\alpha}{2} C'_2 \\ &\quad + (l_i + \lambda C_g) \left(\sqrt{\frac{\rho}{2}} + C_g \sqrt{4(1 - 2\beta\rho)^S + \frac{3\beta C'_1}{2\rho}} \right), \end{aligned}$$

where it follows from Lemma 4. If we choose $\alpha = \Theta((1 + \lambda^2)^{-\frac{1}{2}}\gamma^{-\frac{1}{2}}K^{-\frac{1}{2}}T^{-\frac{1}{2}})$, $\rho = \Theta((1 + \lambda^2)\gamma KT^{-1})$, $\beta = \Theta((1 + \lambda^2)^2K^{-1}T^{-2})$, and $S = \Theta((1 + \lambda^2)^{-2}\gamma^{-1}T^3)$, we can get $\frac{1}{T} \sum_{t=0}^{T-1} \mathbb{E}[\|G(\theta_t)w_{t,\lambda}^* + \lambda G_0(\theta_t)\|^2]$

$= \mathcal{O}((1 + \lambda^2)K^{\frac{1}{2}}\gamma^{\frac{1}{2}}T^{-\frac{1}{2}})$. Furthermore, by choosing λ as constant and following the same step as in Appendix C.3, we have

$$\frac{1}{T} \sum_{t=0}^{T-1} \mathbb{E}[\|G(\theta_t)w_t^*\|^2] = \mathcal{O}(K^{\frac{1}{2}}\gamma^{\frac{1}{2}}T^{-\frac{1}{2}}).$$

To achieve an ϵ -accurate Pareto stationary point, it requires $T = \mathcal{O}(K\gamma\epsilon^{-2})$. In this case, each objective requires a similar number of samples $\mathcal{O}(K^4\gamma^3\epsilon^{-8})$ in ξ (ξ') and $\mathcal{O}(K\gamma\epsilon^{-2})$ samples in ζ , respectively. As far as we know, this is the first provable objective sampling strategy for stochastic multi-objective optimization. \square

D Detailed proofs for convergence analysis under bounded function assumption

D.1 Proof of Theorem 3

Theorem 7 (Restatement of Theorem 3). *Suppose Assumption 1-3 are satisfied and there exists a constant $F > 0$ such that $\forall t \in [T]$, $\|L(\theta_t)\| \leq F$. Set $\alpha = \mathcal{O}((1 + \lambda^2)^{-\frac{1}{2}}K^{-\frac{1}{2}}T^{-\frac{1}{2}})$ and $\beta = \mathcal{O}((1 + \lambda^2)^{-\frac{1}{2}}K^{-1}T^{-1})$. The iterates of the proposed SDMGrad algorithm satisfy,*

$$\frac{1}{T} \sum_{t=0}^{T-1} \mathbb{E}[\|G(\theta_t)w_{t,S} + \lambda G_0(\theta_t)\|^2] = \mathcal{O}((1 + \lambda)^2 K^{\frac{1}{2}} T^{-\frac{1}{2}}).$$

Proof. Now we define a new function, for any i ,

$$L'_i(\theta_t) = L_i(\theta_t) + \lambda L_0(\theta_t). \quad (33)$$

Then for this new function, we have

$$L'_i(\theta_{t+1}) \leq L'_i(\theta_t) + \alpha_t \langle g_i(\theta_t) + \lambda G_0(\theta_t), -d \rangle + \frac{l'_{i,1} \alpha_t^2}{2} \|d\|^2.$$

where $l'_{i,1} = l_{i,1} + \lambda \max_i l_{i,1}$. Then by multiplying $w_{i,t,S}$ on both side and summing over all $i \in [K]$, we have

$$L'(\theta_{t+1})w_{t,S} \leq L'(\theta_t)w_{t,S} + \alpha_t \langle G(\theta_t)w_{t,S} + \lambda G_0(\theta_t), -d \rangle + \frac{\bar{L}' \alpha_t^2}{2} \|d\|^2 \quad (34)$$

where $\bar{L}' = \max_i l'_i$. For the second term on the RHS, conditioning on θ_t and taking expectation, we have

$$\begin{aligned} & \mathbb{E}[\langle G(\theta_t)w_{t,S} + \lambda G_0(\theta_t), -d \rangle] \\ &= \mathbb{E}[\langle G(\theta_t)w_{t,S} + \lambda G_0(\theta_t), -G(\theta_t)w_{t,S} - \lambda G_0(\theta_t) \rangle] \\ &= -\mathbb{E}[\|G(\theta_t)w_{t,S} + \lambda G_0(\theta_t)\|^2]. \end{aligned} \quad (35)$$

Then take expectation on eq. (34), substitute eq. (25) and eq. (35) into it and unconditioning on θ_t , we can obtain

$$\mathbb{E}[L'(\theta_{t+1})w_{t,S}] \leq \mathbb{E}[L'(\theta_t)w_{t,S}] - \alpha_t \mathbb{E}[\|G(\theta_t)w_{t,S} + \lambda G_0(\theta_t)\|^2] + \frac{\bar{L}' \alpha_t^2}{2} C_2.$$

Rearranging this inequality, choosing $\alpha_t = \alpha$ and telescoping over $t \in [T]$ yield

$$\sum_{t=0}^{T-1} \alpha \mathbb{E}[\|G(\theta_t)w_{t,S} + \lambda G_0(\theta_t)\|^2] \leq \sum_{t=0}^{T-1} \mathbb{E}[L'(\theta_t)w_{t,S} - L'(\theta_{t+1})w_{t,S}] + \frac{\bar{L}'\alpha^2}{2}C_2T. \quad (36)$$

Then for the first term on the RHS, we have

$$\begin{aligned} \sum_{t=0}^{T-1} \mathbb{E}[L'(\theta_t)w_{t,S} - L'(\theta_{t+1})w_{t,S}] &= \mathbb{E}\left[\sum_{t=0}^{T-2} (L'(\theta_{t+1})(w_{t+1,S} - w_{t,S}) + L'(\theta_0)w_{0,S} \right. \\ &\quad \left. - L'(\theta_T)w_{T-1,S})\right] \\ &\stackrel{(i)}{\leq} \mathbb{E}\left[\sum_{t=0}^{T-2} F'\beta_t\|G(\theta_t; \xi)^T(G(\theta_t; \xi')w_{t,S} + \lambda G_0(\theta_t; \xi')) \right. \\ &\quad \left. + \rho w_{t,S}\| + 2F'\right] \\ &\stackrel{(ii)}{\leq} \beta F'(T-1)\sqrt{3C_1} + 2F'. \end{aligned} \quad (37)$$

where (i) follows from the bounded function value assumption, (ii) follows from eq. (17) with $\beta_t = \beta$, and $F' = F + \lambda F$. Then substitute eq. (37) into eq. (36), we have

$$\frac{1}{T} \sum_{t=0}^{T-1} \mathbb{E}[\|G(\theta_t)w_{t,S} + \lambda G_0(\theta_t)\|^2] \leq \frac{\beta F'(T-1)\sqrt{3C_1}}{\alpha T} + \frac{2F'}{\alpha T} + \frac{\bar{L}'\alpha}{2}C_2$$

Since $C_1 = \mathcal{O}(K^2 + \lambda^2 K^2)$, $C_2 = \mathcal{O}(K + \lambda^2 K)$, $F' = \mathcal{O}(1 + \lambda)$ and $\bar{L}' = \mathcal{O}(1 + \lambda)$, if we choose $\alpha = \Theta((1 + \lambda^2)^{-\frac{1}{2}} K^{-\frac{1}{2}} T^{-\frac{1}{2}})$ and $\beta = \Theta((1 + \lambda^2)^{-\frac{1}{2}} K^{-1} T^{-1})$, we have

$$\frac{1}{T} \sum_{t=0}^{T-1} \mathbb{E}[\|G(\theta_t)w_{t,S} + \lambda G_0(\theta_t)\|^2] = \mathcal{O}((1 + \lambda)^2 K^{\frac{1}{2}} T^{-\frac{1}{2}}).$$

The proof is complete. □

D.2 Proof of Corollary 3

Proof. Similarly to Appendix C.3, we can obtain

$$\frac{1}{T} \sum_{t=0}^{T-1} \mathbb{E}[\|G(\theta_t)w_t^*\|^2] = \mathcal{O}(K^{\frac{1}{2}} T^{-\frac{1}{2}}).$$

To achieve an ϵ -accurate Pareto stationary point, it requires $T = \mathcal{O}(K\epsilon^{-2})$. From Theorem 7, there is no requirement on the number of w updates. Thus, we can choose S as a constant number such that each objective requires $\mathcal{O}(K\epsilon^{-2})$ samples in ξ (ξ') and $\mathcal{O}(K\epsilon^{-2})$ samples in ζ , respectively. □

D.3 Proof of Theorem 4

Theorem 8 (Restatement of Theorem 4). *Suppose Assumption 1-3 are satisfied and there exists a constant $F > 0$ such that $\forall t \in [T]$, $\|L(\theta_t)\| \leq F$. Set $\gamma = \frac{K}{n}$, $\alpha = \Theta\left(\sqrt{\frac{1}{KT\gamma(1+\lambda^2)}}\right)$ and $\beta = \Theta((1 + \lambda^2)^{-\frac{1}{2}}K^{-1}T^{-1}\gamma^{-1})$. The iterates of the proposed SDMGrad-OS algorithm satisfy,*

$$\frac{1}{T} \sum_{t=0}^{T-1} \mathbb{E}[\|G(\theta_t)w_t^*\|^2] = \mathcal{O}(K^{\frac{1}{2}}\gamma^{\frac{1}{2}}T^{-\frac{1}{2}}).$$

Proof. In SDMGrad, the vector for updating θ_t is $d' = \frac{K}{n}H(\theta_t; \zeta)w_{t,S} + \frac{\lambda K}{n}H_0(\theta_t; \zeta)$. Using the same function defined in eq. (33), we have

$$L'_i(\theta_{t+1}) \leq L'_i(\theta_t) + \alpha_t \langle g_i(\theta_t) + \lambda G_0(\theta_t), -d' \rangle + \frac{l'_{i,1}\alpha_t^2}{2} \|d'\|^2.$$

Then by multiplying $w_{i,t,S}$ on both side and summing over all $i \in [K]$, we have

$$L'(\theta_{t+1})w_{t,S} \leq L'(\theta_t)w_{t,S} + \alpha_t \langle G(\theta_t)w_{t,S} + \lambda G_0(\theta_t), -d' \rangle + \frac{\bar{L}'\alpha_t^2}{2} \|d'\|^2 \quad (38)$$

Then taking expectation on eq. (38) and following from eq. (31), we can obtain

$$\mathbb{E}[L'(\theta_{t+1})w_{t,S}] \leq \mathbb{E}[L'(\theta_t)w_{t,S}] - \alpha_t \mathbb{E}[\|G(\theta_t)w_{t,S} + \lambda G_0(\theta_t)\|^2] + \frac{\bar{L}'\alpha_t^2}{2} C'_2.$$

Rearranging the above inequality and following the same step as in eq. (37), we have

$$\frac{1}{T} \sum_{t=0}^{T-1} \mathbb{E}[\|G(\theta_t)w_t + \lambda G_0(\theta_t)\|^2] \leq \frac{\beta F'(T-1)\sqrt{3C'_1}}{\alpha T} + \frac{2F'}{\alpha T} + \frac{\bar{L}'\alpha}{2} C'_2.$$

If we choose $\alpha = \Theta\left(\sqrt{\frac{1}{KT\gamma(1+\lambda^2)}}\right)$ and $\beta = \Theta((1 + \lambda^2)^{-\frac{1}{2}}K^{-1}T^{-1}\gamma^{-1})$, we can get

$$\frac{1}{T} \sum_{t=0}^{T-1} \mathbb{E}[\|G(\theta_t)w_t + \lambda G_0(\theta_t)\|^2] = \mathcal{O}((1 + \lambda)^2 K^{\frac{1}{2}} \gamma^{\frac{1}{2}} T^{-\frac{1}{2}}).$$

Thus by following Appendix C.3 we can obtain

$$\frac{1}{T} \sum_{t=0}^{T-1} \mathbb{E}[\|G(\theta_t)w_t^*\|^2] = \mathcal{O}(K^{\frac{1}{2}}\gamma^{\frac{1}{2}}T^{-\frac{1}{2}}).$$

To achieve an ϵ -accurate Pareto stationary point, it requires $T = \mathcal{O}(K\gamma\epsilon^{-2})$. Also note that there is no requirement on the number of w updates. Thus, we can choose S as a constant number such that each objective requires $\mathcal{O}(K\gamma\epsilon^{-2})$ samples in ξ (ξ') and $\mathcal{O}(K\gamma\epsilon^{-2})$ samples in ζ , respectively. Then, the proof is complete. \square